

NUREG/CR-2760
ARL-48-82
SAND82-7063

Assessment of Scale Effects on Vortexing, Swirl, and Inlet Losses in Large Scale Sump Models

Containment Sump Reliability Studies
Generic Task A-43

Prepared by M. Padmanabhan, G. E. Hecker/ARL

Alden Research Laboratory
Worcester Polytechnic Institute

Sandia National Laboratories

Prepared for
U.S. Nuclear Regulatory
Commission

NOTICE

This report was prepared as an account of work sponsored by an agency of the United States Government. Neither the United States Government nor any agency thereof, or any of their employees, makes any warranty, expressed or implied, or assumes any legal liability of responsibility for any third party's use, or the results of such use, of any information, apparatus, product or process disclosed in this report, or represents that its use by such third party would not infringe privately owned rights.

Availability of Reference Materials Cited in NRC Publications

Most documents cited in NRC publications will be available from one of the following sources:

1. The NRC Public Document Room, 1717 H Street, N.W.
Washington, DC 20555
2. The NRC/GPO Sales Program, U.S. Nuclear Regulatory Commission,
Washington, DC 20555
3. The National Technical Information Service, Springfield, VA 22161

Although the listing that follows represents the majority of documents cited in NRC publications, it is not intended to be exhaustive.

Referenced documents available for inspection and copying for a fee from the NRC Public Document Room include NRC correspondence and internal NRC memoranda; NRC Office of Inspection and Enforcement bulletins, circulars, information notices, inspection and investigation notices; Licensee Event Reports; vendor reports and correspondence; Commission papers; and applicant and licensee documents and correspondence.

The following documents in the NUREG series are available for purchase from the NRC/GPO Sales Program: formal NRC staff and contractor reports, NRC-sponsored conference proceedings, and NRC booklets and brochures. Also available are Regulatory Guides, NRC regulations in the *Code of Federal Regulations*, and *Nuclear Regulatory Commission Issuances*.

Documents available from the National Technical Information Service include NUREG series reports and technical reports prepared by other federal agencies and reports prepared by the Atomic Energy Commission, forerunner agency to the Nuclear Regulatory Commission.

Documents available from public and special technical libraries include all open literature items, such as books, journal and periodical articles, and transactions. *Federal Register* notices, federal and state legislation, and congressional reports can usually be obtained from these libraries.

Documents such as theses, dissertations, foreign reports and translations, and non-NRC conference proceedings are available for purchase from the organization sponsoring the publication cited.

Single copies of NRC draft reports are available free upon written request to the Division of Technical Information and Document Control, U.S. Nuclear Regulatory Commission, Washington, DC 20555.

Copies of industry codes and standards used in a substantive manner in the NRC regulatory process are maintained at the NRC Library, 7920 Norfolk Avenue, Bethesda, Maryland, and are available there for reference use by the public. Codes and standards are usually copyrighted and may be purchased from the originating organization or, if they are American National Standards, from the American National Standards Institute, 1430 Broadway, New York, NY 10018.

NUREG/CR-2760
ARL-48-82
SAND82-7063

Assessment of Scale Effects on Vortexing, Swirl, and Inlet Losses in Large Scale Sump Models

Containment Sump Reliability Studies
Generic Task A-43

Manuscript Completed: May 1982
Date Published: June 1982

Prepared by
M. Padmanabhan, G. E. Hecker, Alden Research Laboratory

Alden Research Laboratory
Worcester Polytechnic Institute
Holden, MA 01520

Sandia National Laboratories
Albuquerque, NM 87185

Prepared for
Division of Safety Technology
Office of Nuclear Reactor Regulation
U.S. Nuclear Regulatory Commission
Washington, D.C. 20555
NRC FIN A1296

ABSTRACT

To verify the use of reduced scale hydraulic models of large scale ratios to demonstrate the performance of containment emergency sumps, in view of concerns regarding possible scale effects, a test program involving two geometric scale models (1:2 and 1:4) of a full size sump (1:1) was undertaken as a part of the total test program towards the resolution of unresolved safety issue A-43, "Containment Emergency Sump Performance".

The test results substantiated that hydraulic models with large scales such as 1:2 to 1:4 reliably predicted the sump hydraulic performance; namely, vortexing, air-ingestion from free surface vortices, pipe flow swirl and inlet loss coefficient. No scale effects on vortexing or air-withdrawals were apparent within the tested prediction range for both models. However, a good prediction of pipe flow swirl and inlet loss coefficient was found to require that the approach flow Reynolds number and pipe Reynolds number be above certain limits.

Based on the results of these tests, it is concluded that properly designed and operated reduced scale hydraulic models of geometric scales 1:4 or larger can be used both by utilities and by regulatory agencies to prove the satisfactory hydraulic performance of a sump design. The reliability of predictions made by model studies conducted in the past may be evaluated by comparing the hydraulic operating parameters of the models to the criteria given herein, and to other published criteria.

TABLE OF CONTENTS

	<u>Page No.</u>
ABSTRACT	iii
LIST OF FIGURES	vii
LIST OF TABLES	ix
ACKNOWLEDGEMENTS	xi
EXECUTIVE SUMMARY	1
1.0 INTRODUCTION	4
2.0 TEST DETAILS	6
2.1 Objectives of the Program	6
2.2 Test Configuration	6
2.3 Test Plan	8
2.4 Test Durations	12
3.0 KEY FINDINGS SUMMARY	14
4.0 DETAILED RESULTS	17
4.1 Vortexing	18
4.2 Air-withdrawals Due to Vortices	27
4.3 Pipe Swirl	27
4.4 Inlet Losses	40
4.5 Blockage Tests With No Screens and Gratings in the Unblocked Screen Area	44
4.6 Envelope Curves	44
4.7 General	50
REFERENCES	51
APPENDIX A - FACILITY, MEASUREMENT TECHNIQUES AND DATA ACQUISITION	A1
APPENDIX B - MODEL SIMILITUDE	B1

LIST OF FIGURES

	PAGE
1	Geometric parameters of selected sump (1:1) 7
2	Screen blockage schemes tested for scale model tests 13
3	Average vortex type data for uniform approach flow, both pipes operating, tests 19
4	Average vortex type data for one pipe only tests, $s/d = 2.5$ 20
5	Average vortex type data for screen blockage tests; $s/d = 2.5$; both pipes operating 21
6	Persistence of vortices for models and prototype 22
7	Device for angular velocity measurement 23
8	Average vortex types for various radial Reynolds numbers; uniform approach flow; both pipes operating 25
9	Typical sub-surface vortices (submerged vortices) in scale models; uniform approach flow; both pipes operating; $s/d = 3$, $F = 0.47$, $d = 12"$ for 1:2 and 6" for 1:4 model 26
10	Air-withdrawals due to air-core vortices for the scale models tested with screen blockage scheme 2; $s/d = 2.5$ 28
11	Swirl angle data for various submergences; 1:1 scale model; uniform approach flow; both pipes operating 30
12	Swirl angle data for various submergences; 1:2 scale model; uniform approach flow; both pipes operating 31
13	Swirl angle data for various submergences; 1:4 scale model; uniform approach flow; both pipes operating 32
14	Swirl angle versus Froude number; one pipe operating; $s/d = 2.5$ 33

LIST OF FIGURES (Cont)

		PAGE
15	Swirl angle variation with Froude number; screen blockages; pipe 2 data; $s/d = 2.5$	34
16	Variation of ratio of measured swirl angles to average prototype measured swirl angle with approach flow Reynolds number, uniform approach flow, both pipes operating	36
17	Variation of ratio of measured swirl angles to average prototype measured swirl angle with approach flow Reynolds number, one pipe operating	37
18	Variation of ratio of measured swirl angles to average prototype measured swirl angle with approach flow Reynolds number, screen blockage scheme 2	38
19	Variation of ratio of measured swirl angles to average prototype measured swirl angle with approach flow Reynolds number; all data for $s/d = 2.5$ included	39
20	Variation of the ratio of swirl angles near inlet to average prototype swirl angle near inlet with approach flow Reynolds number; all data for $s/d = 2.5$	41
21	Inlet loss coefficient versus Froude number; uniform approach flow; both pipes operating	42
22	Inlet loss coefficient variation with pipe Reynolds number; both pipes operating; uniform flow; pipe 1 data	43
23	Inlet loss coefficient versus pipe Reynolds number; screen blockage scheme 2; $s/d = 2.5$; pipe 2	45
24	Inlet loss coefficient variation with pipe Reynolds number; one pipe operating; $s/d = 2.5$	46
25	Results of tests with no screens and gratings in open portion of scheme 2 blockage	47
26	Average vortex type data compared with respect to envelope line from phase 1, tests (7)	48
27	Void fraction data compared with respect to envelope line from phase 1, tests (7)	49

LIST OF TABLES

		PAGE
1	Test plan for scale model tests	9
2	Flows and submergences in models	11
3	Summary of significant findings regarding scale effects	16
4	Detailed results	17
5	Measured angular velocities*	24

ACKNOWLEDGEMENTS

This research program was funded by the U.S. Department of Energy (DOE), and their support is sincerely appreciated. The scope of work was developed with significant technical contributions made by personnel from the U.S. Nuclear Regulatory Commission (NRC) and Sandia National Laboratories (Sandia), and the efforts of these organizations are gratefully acknowledged. Particular thanks are due to Mr. Andrew Millunzi of DOE, Mr. Aleck Serkiz of the NRC, and Messrs. Peter Strom and Gilbert Weigand of Sandia for their efforts and valuable contributions.

The help provided by all members of the staff at the Alden Research Laboratory associated with this research project is gratefully acknowledged. Special mention must be made of the actual conduct of experiments by Messrs. John Noreika and Russell Dube, the designing of required facility modifications by Mr. Dean K. White, and computer programming and graphics by Dr. S.K. Hsu.

NOMENCLATURE

c	Distance of pipe center from sump floor
C_L	Inlet loss coefficient
d	Pipe internal diameter
d_w	Diameter of screen wire
E	Euler number, $u/\sqrt{\Delta p/\rho}$
F	Froude number, u/\sqrt{gs}
F_i	Inertia force
F_p	Pressure force
F_g	Gravity force
F_v	Viscous force
F_t	Surface tension force
g	Acceleration due to gravity
ΔH	Pressure head difference
K	Pressure drop coefficient for screen; constant of proportionality
L	Length, linear dimension
n	Number of revolutions/sec for swirl meter
Δp	Pressure drop
Q	Flow in each pipe
R	Reynolds number
R_a	Approach flow Reynolds number, $u_a s_a/\nu$
R_e	Pipe Reynolds number, ud/ν
R_R	Radial Reynolds number, $Q/\nu s$

R_{Ra}	Radial Reynolds number based on approach flow depth, Q/vs_a
R_s	Screen Reynolds number, $u'_a d_w/v$
s	Submergence of pipe center from water surface
s_a	Depth of approach flow at containment floor close to sump
S'	Solidity ratio of screen
T	Vortex type
t	Time
u	Average axial velocity in the pipe, $Q/\text{Area of pipe cross section}$
u_a	Average velocity of approach flow above the containment floor close to the sump floor depression (see Figure 1)
u'_a	Mean velocity of approach flow upstream of screens
W	Weber number
W_d	Weber number using pipe diameter, $\rho u^2 d/\sigma$
W_s	Weber number using submergence, $\rho u^2 s/\sigma$
x	Axial distance along pipe
Δx	Incremental distance
$\alpha_1, \alpha_2,$ etc.	Proportionality factors
β	Decay factor for swirl
γ	Specific weight of water
σ	Surface tension of water to air
μ	Dynamic viscosity of water
ρ	Density of water
ν	Kinematic viscosity of water
θ	Measured swirl angle
θ_a	Average measured swirl angle for full scale sump

θ_i	Calculated swirl angle close to pipe inlet
$(\theta_i)_a$	Average calculated swirl angle close to pipe inlet for full scale sump
ω_m, ω_p	Angular velocity in reduced scale, full scale

SUFFIXES

P, p	Pertaining to full scale sump
m	Pertaining to model (or reduced scale sumps)
r	Indicating ratio of model to full scale

EXECUTIVE SUMMARY

Hydraulic models of large scales are often used to demonstrate the hydraulic performance of containment sumps, and a knowledge of the reliability of model results, particularly in view of concerns for possible scale effects, is important to the applicant and regulatory agencies. Hence, the hydraulic performance of geometrically scaled models of a full size sump was investigated and model test results were compared with results from the full size sump.

This investigation of possible scale effects was a part of the overall full scale tests of flow conditions in containment recirculation sumps for nuclear power stations conducted at the Alden Research Laboratory (ARL) of Worcester Polytechnic Institute (WPI) for the U.S. Department of Energy (DOE) and the U.S. Nuclear Regulatory Commission (NRC) on a contract from Sandia National Laboratories (Sandia). The overall ARL program is designed to provide sump hydraulic design and performance data for use in resolving the unresolved Safety Issue, Task-43, "Containment Emergency Sump Performance".

The objectives of the scale model investigation are: (a) to examine possible scale effects on vortexing, air-withdrawals due to vortices, pipe flow swirl levels, and inlet loss coefficients, (b) to suggest criteria in designing and operating models to minimize scale effects, and (c) to provide information for the regulatory agency (NRC) to facilitate a review of hydraulic models results used for evaluating sumps.

Two geometric scale models, 1:2 and 1:4, of a rectangular sump (20' x 10' x 4.5' deep) with two horizontal 24 inch outlet pipes at 16 ft spacing were tested in addition to the full size (1:1) sump. The test results have been used to evaluate any scale effects in modeling free surface vortexing, pipe swirl, air-withdrawals due to vortices, and inlet losses. Tests were conducted at selected flows and submergences (scaled conforming to Froude law for the models) for one and two pipe operations with approximately uniform approach flows and for a few cases with sump screen blockages. A few tests of the scale models were conducted with pipe velocities exaggerated to prototype velocities to investigate the so-called "Equal Velocity Rule."

The tests under Froude scaled conditions covered a range of Froude numbers from 0.2 to 0.6, a range of pipe Reynolds numbers from 7.4×10^4 to 9×10^5 , and a range of radial Reynolds numbers from 1.5×10^4 to 2.9×10^5 .

The principal findings may be summarized as follows:

1. Air-withdrawals Due to Vortices

Within the accuracy of measuring low void fractions, the void fractions predicted by both the models were approximately the same as those for the full scale sump. Observed air-core vortices were weak even with asymmetrical screen blockages, producing less than 1% void fractions at the measurement locations. These data indicate there are no significant scale effects in modeling air-core vortices within the range of the Reynolds numbers tested.

2. Vortex Types

Both the 1:2 and 1:4 scale models predicted the average vortex types and the persistence of vortices of various strength very well, indicating no significant scale effects for this phenomenon. Angular velocity measurements at corresponding distances from a stable surface air-core vortex in the models and in the full scale sump indicated that the circulation associated with a free surface vortex is scaled by Froude models.

3. Swirl

Swirl intensity of flow in the pipe appeared to be influenced more by submerged vortices and flow patterns at the pipe entrances than by free-surface vortices. Below an approach flow Reynolds number in the model of about 3.0×10^4 , the models predicted noticeably lower swirl than that in the full scale sump. These data indicate that models should be designed to have an approach flow Reynolds number of 3.0×10^4 or greater if the pipe inlet flow swirl is to be accurately determined.

4. Inlet Losses

The inlet loss coefficients also appeared to be influenced by the Reynolds number, as previously published. Above a model pipe Reynolds number of about 1×10^5 , the full scale inlet loss coefficient was well predicted by the tested hydraulic models.

5. Testing at Higher Flows

Even though reduced scale model tests at velocities above Froude scaled values were not found necessary for prediction of free surface vortices and consequent air-withdrawals, such higher flows may be useful to achieve higher Reynolds numbers in the model for better prediction of pipe swirl and inlet losses.

Based on the test results, it is concluded that a properly designed hydraulic model is a reliable method of predicting the hydraulic performance of containment sumps. No scale effects on vortexing or air-withdrawals due to vortices were apparent. However, it is recommended that the model approach flow Reynolds number exceed 3.0×10^4 , and the model pipe Reynolds number exceed 1.0×10^5 for a reliable prediction of pipe flow swirl and inlet losses, respectively.

These conclusions indicate that the present practice of using reduced scale hydraulic models of scales, such as 1:2 to 1:4, to verify the hydraulic performance of containment sumps is an acceptable procedure. This fact is considered to be an important step towards the resolution of Unresolved Safety Issue, A-43, "Containment Emergency Sump Performance", as hydraulic modeling provides an accurate and efficient means of investigating special cases not conforming to proposed regulatory guidelines (23). Previous hydraulic model studies of containment sumps could be evaluated, relative to their reliability in predicting full scale hydraulic phenomena, by using the criteria developed from the present study, and by using pertinent information available from existing literature (10, 11, 12, 20).

1.0 INTRODUCTION

In the event of a Loss of Coolant Accident (LOCA) in a nuclear power station, the Emergency Core Cooling System (ECCS) and Containment Spray System (CSS) would be activated to supply coolant to the reactor core and vessel to dissipate the decay heat and to the containment building spray system to reduce containment pressure. At first, these systems draw water from a large supply tank. Later, they are switched to a recirculating mode, drawing water that has accumulated in the containment through a containment recirculation sump. Containment recirculation sumps are designed to collect water and supply it to the safety system pumps, to screen out debris, and to provide sufficient suction head for the pumps. Hence, they form a key flow link in providing coolant to the reactor and in providing control of the containment environment during the extended recirculation mode.

The flow patterns within the containment sump influence the character of the flow in suction lines leading to the safety system pumps. Of considerable concern is the tendency for air-entraining vortices to form, either because of the approach flow pattern, or because of swirl initiated by asymmetrical debris blockage of screens. It has been found that air concentrations greater than about 3 percent by volume in a suction line can lower the head-discharge curves of centrifugal pumps considerably, causing lower pump capacities at given head (1, 2, 3). Additionally, large flow swirl intensities and high inlet losses that would reduce the available Net Positive Suction Head (NPSH) at the pumps might also contribute to poor sump performance.

In the experimental evaluation of containment sumps, it is not possible to test the power station under fully simulated accident conditions. It is often not possible to use the full containment floor, but only a blocked-off portion so that approach flow conditions are not fully represented. Further testing at elevated temperature with various screen blockages, investigating possible remedial appurtenances, and measuring all pertinent data, is not usually feasible. The trend, then, has been to conduct full scale experiments in separate facilities or reduced scale model tests based on Froude number similitude, generally at geometric scale of 1:4 and larger, in order to minimize scale effects due to viscous and surface tension forces (4, 5).

Several advantages accrue from the application of a scale model to assure proper sump performance. Model geometry is easily modified such that various approach flow distributions and screen and grating blockages may be simulated easily and quickly. Construction materials and techniques can be used such that flow patterns can be observed throughout the model and instrumentation can be located in all areas of interest, both of which are difficult or impossible with in-situ measurements. Also, remedial measures can be evaluated at minimal expenditure of time and cost.

Many utilities responsible for demonstrating proper sump performance for plants under operation or construction have demonstrated the hydraulic performance of the sumps using reduced scale models. Hence, a better knowledge of the reliability of model results in view of the concerns for scale effects is considered valuable to the licensing authorities at the NRC.

The parameters which directly affect sump performance and vortex suppression were studied experimentally at full scale at the Alden Research Laboratory (ARL) of Worcester Polytechnic Institute (WPI) under a contract from the Sandia National Laboratories (Sandia) on behalf of the U.S. Department of Energy (DOE) for the Resolution of Unresolved Safety Issues, Generic Task A-43, Containment Sump Reliability, under the Light Water Reactor Safety Research and Development Program. This program has been completed and the results are presented in separate reports (6, 7, 8). To examine possible scale effects on air-withdrawals due to vortices, types of vortices, pipe swirl, and inlet losses in models operated based on Froude similitude, limited tests simulating a selected sump to geometric scales of 1:2 and 1:4 were included in the program. These tests were conducted using the full scale facility by suitable modifications to simulate the selected sump geometry to the reduced scales. A test plan was developed with the objective of providing a ready comparison of hydraulic performance of the models operated under Froude law of similitude with that of 1:1 setup for a range of flows and submergences normally encountered in such sumps. A few tests with up to 75% blocked sump screens were included in the test plan to get stronger vortices for comparison purposes. Also, the usefulness of the "equal velocity rule" or operating the model at higher than Froude scaled flows was investigated.

This report presents the test results of the scale models and corresponding full scale sump and the results are compared and discussed so as to evaluate any scale effects observed. Section 3.0 gives a key findings summary outlining the major conclusions and section 4.0 provides the detailed test results including discussion of results based on the available literature on vortexing and Froude similitude modeling.

Descriptions of the test facility, instrumentation, measuring techniques and data acquisition system are all given in detail in references 6 and 21. However, for convenience, a brief description is included in Appendix A. Based on available literature, discussions on Froude similitude, scale effects in vortexing, similarity of vortex motion, and similarity of flow through gratings and screens are given in Appendix B.

2.0 TEST DETAILS

2.1 Objectives of the Program

The following are the objectives of the test program involving full scale and reduced geometric scale models of a containment recirculation sump configuration:

- a. To examine possible scale effects of modeling air-withdrawals due to vortices, the persistence of various types of vortices, pipe flow swirl levels, and pipe inlet loss coefficients, as determined by large scale models with 1:2 and 1:4 scale ratios.
- b. To suggest criteria in designing the models and selecting geometric scales, and applicable limits in operating such models, such that any scale effects are absent or minimal.
- c. To provide data for regulatory agencies (NRC) and license applicants (utilities) to determine whether or not reduced scale hydraulic models are reliable tools for evaluating the hydraulic performance of ECCS recirculation sumps.

2.2 Test Configuration

Figure 1 shows the selected prototype geometric configuration (1:1 scale) which is a 20 ft x 10 ft sump, 6 ft deep with two 24 inch horizontal outlet pipes at 16 ft centers. This configuration is within the range of typical geometries of existing or planned sumps and was chosen so that the scale models could be built in the same facility with least cost and time, using false floors and walls and scaled outlet pipe of standard dimensions. The locations of the swirl meter and the gradient pressure taps from the pipe inlet were scaled for the 1:4 model; namely, about 8 pipe diameters to the swirl meter and 18 pipe diameters to the first pressure tap, with 10 taps at every 1 pipe diameter thereafter. For the 1:2 model, the pressure tap locations were scaled, but the swirl meter was located 11 pipe diameters from pipe inlet due to piping constraints in the facility.

The full scale screens were used in the models, which gave essentially the same screen loss coefficients in the models at their screen Reynolds numbers as was the case in the full scale facility. For the gratings, the depth and spacings of the bars were exactly modeled to the geometric scale, while the thickness of the bars was higher than scaled values in the models. The model gratings were fabricated at ARL from plexiglass. Some tests were done without any bars or screens in place in the unblocked areas so as to remove influence of scaling these items.

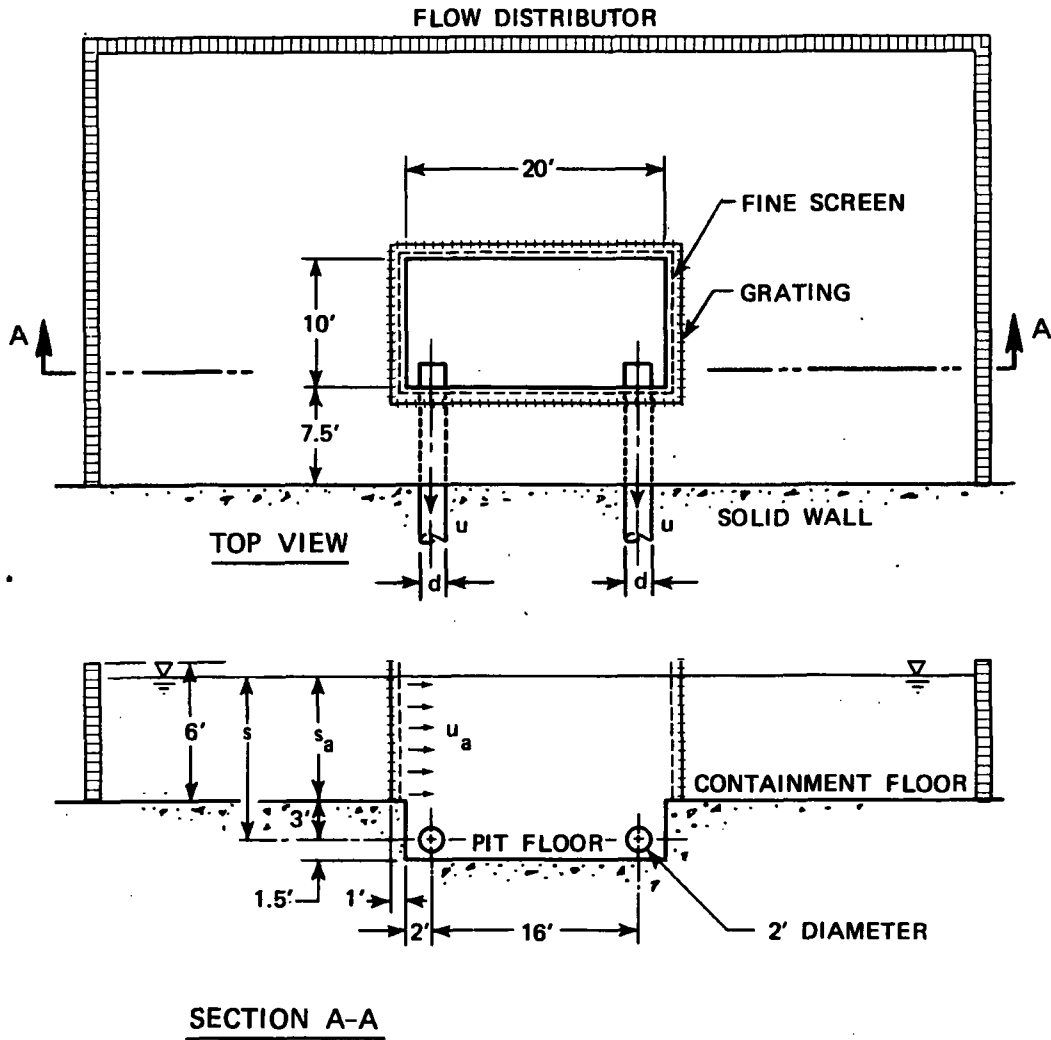


FIGURE 1 GEOMETRIC PARAMETERS OF SELECTED SUMP (1:1)

2.3 Test Plan

A test plan (Table 1) was designed to attain the main objective of the tests; namely, to ascertain any possible scale effects on vortex types, air-withdrawals due to vortices, swirl in pipe flow and inlet loss coefficient as predicted by the scale models operated according to Froude similitude, while at the same time keeping the test plan concise and within the available time and funds.

A. Uniform Approach Flow Tests

In these tests, the approach flow was allowed to reach the sump more or less uniformly from all sides, with no intentional flow perturbations applied. These tests conform to the majority of tests involved in the full scale parametric study (6, 7). The tests were conducted with both pipes operating at Froude scaled flows corresponding to prototype flows of 5300, 6600, 8000, and 9000 gpm/pipe, at scaled submergences corresponding to 5, 6, and 8 ft of water from the pipe center. For the submergence corresponding to 5 ft, the scale model tests were repeated at "equal velocity" flows, which means the flow was increased to values giving the full scale pipe velocity, keeping the scaled submergence. Table 2 shows the scaled and "equal velocity" flows and submergences.

Since even slight approach flow distribution variations affect circulation and vortexing, special care was taken to set the flows in each outlet pipe as close to the established values as possible. Also, the return flow to the facility was carefully measured in each line and divided equally between the inflow lines. A divider wall was installed half-way around the supply trench upstream of the flow distributor to achieve a repeatable and uniform flow toward the sump. Even with this extra effort, it was realized that it would be difficult to obtain exactly the same approach flow pattern for each model as with the full scale sump, and the location of the maximum vortex might occur at differing pipe inlets.

B. One-Pipe Operation Tests

With one pipe operating in the selected double-outlet sump a single vortex could be expected to form at a consistent location, thereby avoiding the problem of collecting data on more than one vortex of the same strength intermittently occurring at different locations. These tests were conducted only for scaled flows corresponding to full size flows of 5300, 6600, 8000, and 9000 gpm at a scaled submergence corresponding to 5 ft. The approach flow to the sump was made as uniform as possible, as described above.

TABLE 1

Test Plan For Scale Model Tests

A. Uniform Approach Flow Tests (both pipes operational)

(i) Scaled Flows

Corresponding to full scale flows:

$$Q_p = 5,300, 6,600, 8,000, \text{ and } 9,000 \text{ gpm/pipe}$$

Corresponding to full scale submergences:

$$S_p = 5, 6, \text{ and } 8 \text{ ft}$$

(ii) Equal Velocity Rule Flows

Corresponding to full scale flows:

$$Q_p = 5,300, 6,600, 8,000, \text{ and } 9,000 \text{ gpm/pipe}$$

Corresponding to full scale submergences:

$$S_p = 5 \text{ ft only}$$

B. "One-Pipe Only" Tests

Scaled flows corresponding to full scale flows for $S_p = 5$ ft only
(5,300 to 9,000 gpm)

C. Selected Screen Blockage Tests

Selected two screen blockages (schemes 1 and 2) that give air-core vortices in 1:4 model (by trial), for each blockage perform:

- (i) tests at scaled flows for $S_p = 5$ ft only (5,300 to 9,000 gpm/pipe),
- (ii) tests at equal velocity flows for $S_p = 5$ ft only for blockage scheme 2.

D. "No-Grating: No Screen" Tests

For screen blockage scheme 2, repeat tests without grating and screens in the open portion of screen cage, for $S_p = 5$ ft only, at scaled and equal velocity flows corresponding to two flows (6,600 and 9,000 gpm/pipe).

E. Test Durations

	<u>Full Scale</u>	<u>1:2 Scale</u>	<u>1:4 Scale</u>
Total Test Time	60 min.	40 min.	30 min.
Vortex Observation Interval*	30 sec.	20 sec.	15 sec.

*When both pipes are drawing strong vortices, observations are made alternately on each pipe. Otherwise, the stronger vortex at a given pipe is observed continuously.

TABLE 2
Flows and Submergences in Models

FROUDE SCALED FLOWS

<u>Full Scale Flow, Q_p gpm</u>	<u>1:2 Model Flow gpm</u>	<u>1:4 Model Flow gpm</u>
5300	937	166
6600	1167	206
8000	1414	250
9000	1591	281

FROUDE SCALED SUBMERGENCES

<u>Full Scale Submergence, S_p ft</u>	<u>1:2 Model Submergence ft</u>	<u>1:4 Model Submergence ft</u>
5	2.5	1.25
6	3.0	1.5
8	4.0	2.0

EQUAL VELOCITY FLOWS

<u>Full Scale Flow gpm</u>	<u>1:2 Model gpm</u>	<u>1:4 Model gpm</u>
5300	1325	331
6600	1650	413
8000	2000	500
9000	2250	563

C. Screen Blockage Tests

Two screen blockage schemes with about 75% blockage, that gave air-core vortices at higher flows, were selected using available results from the full scale parametric study on several sump configurations and by trial testing. The selected two blockage schemes, designated as schemes 1 and 2, are illustrated in Figure 2. The screen blockage tests, in general, gave stronger vortexing, swirl and higher inlet losses in the parametric sump study, and a comparison of predicted severities between the models and the full size sump under screen blockages was considered useful. Screen blockage tests also fixed the location of maximum vortex at a given outlet pipe. Scheme 2 gave stronger vortexing and a wide range of vortex types was observed for the tested range of Froude number. Hence, these tests will be used in the discussion of results to evaluate any scale effects. Tests were conducted with both pipes operating at Froude scaled flows corresponding to full size flows of 5300, 6600, 8000, and 9000 gpm/pipes at a submergence corresponding to 5 ft. The approach flow to the sump was made as uniform as possible, as described above.

The screen blockage tests with scheme 2 were also repeated after removing the screen and grating at the open portion, for scaled flows corresponding to 6600 and 9000 gpm/pipe, and a scaled submergence corresponding to 5 ft. These tests were intended to provide data without the secondary influence of possible scale effects due to the scaling of gratings and screens.

2.3 Test Durations

For the 1:4 scale model, a test duration of 30 minutes was chosen, this being a sufficient sampling time as indicated by the earlier full scale parametric studies. Vortices were observed every 15 seconds, concentrating on the stronger vortex. However, if two consistent vortices of essentially the same strength occurred, one at each pipe, each vortex was observed alternately.

For the 1:2 and 1:1 sumps, both the test duration and the observation intervals were increased according to Froude scaling ($t_x = L^{0.5}$), giving a value of about 40 minutes and 20 seconds, respectively, for 1:2 sump, and 60 minutes and 30 seconds, respectively, for 1:1 sump. The swirl angles, void fractions, and inlet loss coefficients were obtained at constant intervals of 30 seconds, 5 seconds, and 60 seconds, respectively, but only test average values were used for evaluating scale effects.

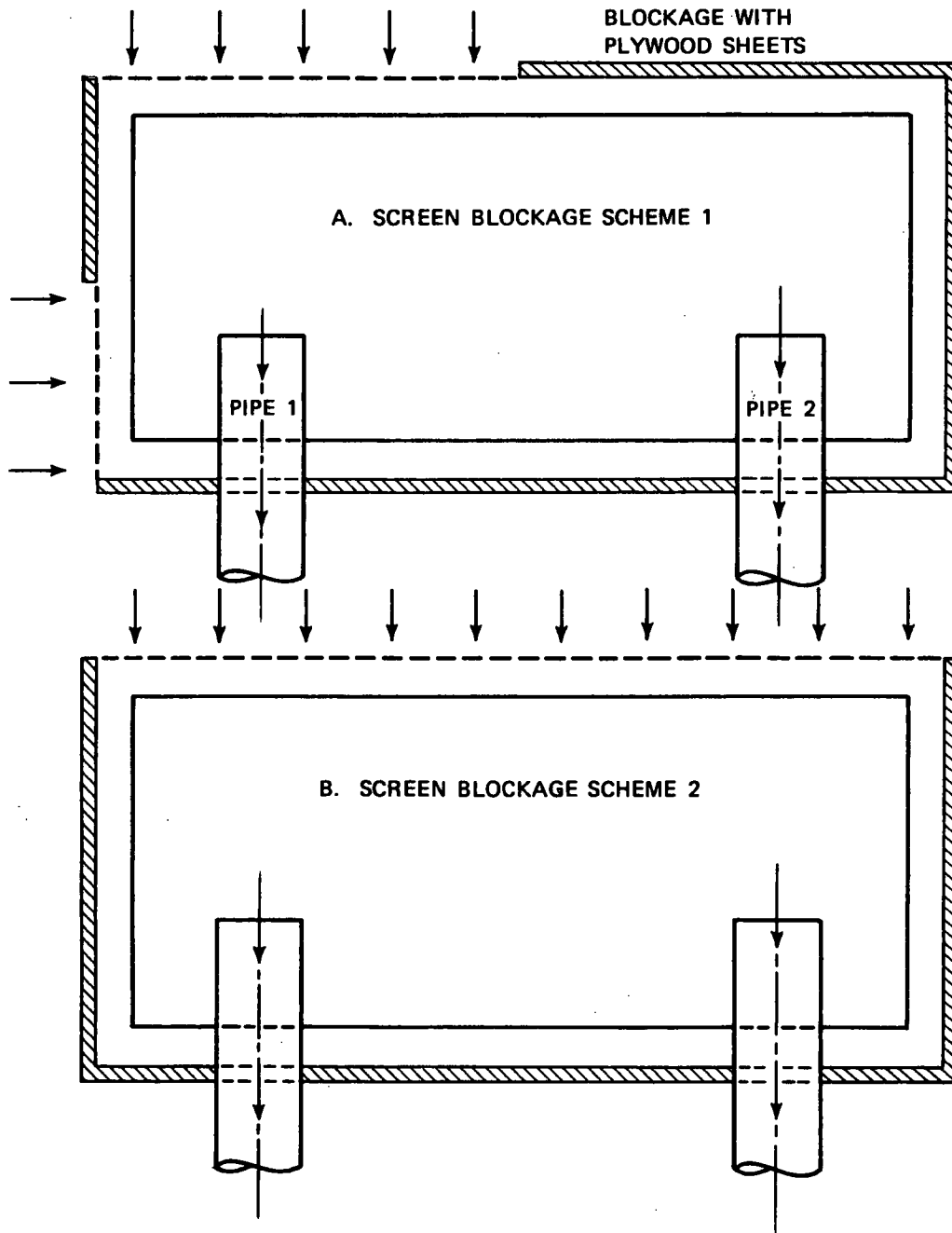


FIGURE 2 SCREEN BLOCKAGE SCHEMES TESTED FOR SCALE MODEL TESTS

3.0 KEY FINDINGS SUMMARY

The results of detailed tests on the 1:4, 1:2, and 1:1 scale versions of the same sump under comparable operating conditions lead to the key findings summarized in the following paragraphs. The tested range of Froude numbers, $u/(gs)^{0.5}$, was 0.2 to 0.6. For the reduced scaled models, the radial Reynolds number (Q/Vs) was above 1.5×10^4 , the pipe Reynolds number (ud/v) was above 7×10^4 , and the Weber number ($\rho u^2 d/\sigma$) was above 600. A summary of the most significant findings regarding possible scale effects is given in Table 3.

- a. When air-core vortices were present, they did not produce any significant air-withdrawals. The measured void fractions were considerably less than 1%, within the accuracy of the void fraction meter. Within this constraint, the reduced scale models predicted the full scale air-withdrawals well. In other words, the models did not indicate any obvious underprediction of air-withdrawals.
- b. No significant scale effects on modeling free-surface vortexing were found in the 1:2 and 1:4 models operated according to Froude similitude. This supports the conclusions on minimal scale effects reported previously (20). Tests included both pipes operating with and without screen blockages and one pipe operation without screen blockages, producing a wide range of vortices, types 2 to 6. Both the average vortex types and the persistence of vortices were predicted well by the reduced scale models.
- c. For the depressed sump configuration (sump floor below the containment floor level) tested, sub-surface vortexing was found to form along the shear layers at the separation region as the flow entered the floor depression. These vortices were identifiable by dye injection, but were unstable and unsteady, particularly in the full scale sump. The submerged vortices contributed to pipe flow swirl, which perhaps served as an indication of the strength of these submerged vortices.
- d. Limited measurements of surface angular velocity at a selected distance from air-core vortices indicated the models scaled angular velocity well. This implies the general flow pattern and circulation in the full scale sump were also scaled properly.
- e. The pipe flow swirl was seen to exhibit some scale effects when the approach flow Reynolds number ($u_a s_a/v$) was below about 3×10^4 (See Figure 1 for definition of u_a and s_a). Hence, it is suggested that reduced scale models have approach flow Reynolds numbers above 3×10^4 in depressed floor sump models if underpredicted by models of pipe swirl measurements is to be avoided. If this is not possible, a correction of measured swirl angles may be possible using Figure 20.

- f. For model pipe Reynolds numbers above 1×10^5 , the full scale inlet losses were predicted well by the reduced scale models. For R_e below 1×10^5 , some Reynolds number effects are probable, since higher loss coefficients were indicated.
- g. Proper model design, selection of a geometric scale, and model operation, required that certain non-dimensional numbers in the model equal or exceed prescribed limits, so as to avoid any significant scale effects. On the basis of the present investigation, no significant scale effects were observed in the model for, (i) Radial Reynolds number Q/Vs above 1.5×10^4 , (ii) Weber number, $\rho u^2 d/\sigma$ above 600, (iii) approach flow Reynolds number, u_s/ν , above 3×10^4 and, (iv) Pipe Reynolds number above 10^5 . Items (i) and (ii) are the lower limits of the present study and may not necessarily be the lower limits for negligible scale effects on free-surface vortexing. Items (iii) and (iv) are derived from the results of the present study and are actual lower limits to minimize scale effects in predicted swirl angles and inlet loss coefficients.
- h. Properly designed hydraulic models, operated based on Froude similitude meeting the above minimum values of dimensionless numbers, is thus a proper means of predicting the hydraulic performance of containment sumps. The practice of using large scale hydraulic models to verify sump designs, both by the applicant and regulatory agencies, is therefore found to be appropriate. Past hydraulic model studies can be evaluated, relative to their reliability in predicting full scale hydraulic phenomena, by comparing the minimum values of dimensionless numbers based on the hydraulic operating parameters in the model to the desired limits of these numbers obtained from this study and other available publications (10, 11, 12).

TABLE 3

Summary of Significant Findings

Regarding Scale Effects

<u>Category</u>	<u>Significant Findings</u>	<u>Reference Figures</u>
Free Surface Vortexing	No scale effects on average vortex types and persistence	Figures 3 to 6
Air Ingestion	Within the measurement accuracies, no scale effects apparent. Magnitudes very small; usually less than 0.2% void fractions.	Figure 10
Pipe Flow Swirl Angles	No scale effects, if model approach flow Reynolds number, $U S_a / \nu$, is above 3×10^4 . For lower Reynolds numbers, swirl magnitude is underpredicted by models. Usual values were about 6 degrees without screen blockages; up to 12.5 degrees with screen blockages.	Figures 16 to 20
Inlet Loss Coefficients	No scale effects if model pipe Reynolds number is above 1×10^5 . For lower Reynolds numbers, inlet losses somewhat overpredicted by models. In general, values were 0.8 to 1.0.	Figures 21 to 24

4.0 DETAILED RESULTS

The results are presented as direct comparisons of model to full scale data considering each item of concern, such as free surface vortex severity, swirl in the pipes, inlet losses, and air-withdrawals due to air-core vortices. Non-dimensional numbers; namely, Froude number, radial Reynolds number, pipe Reynolds number, approach flow Reynolds number, and Weber number commonly used in the literature are used in the discussion of results, as appropriate. The range of these parameters are given in Table 4, and Figure 1 provides the definitions of flow and geometric variables.

TABLE 4
Ranges of Non-Dimensional Numbers

	Geometric Scale		
	1:1	1:2	1:4
Froude number ($F = u/\sqrt{gs}$)	0.2 to 0.6	0.2 to 0.6	0.2 to 0.6
Pipe Reynolds Number ($Re = ud/\nu$)	4.9×10^5 to 9.3×10^5	1.9×10^5 to 3.4×10^5	7.0×10^4 to 1.4×10^5
Radial Reynolds Number ($R_R = Q/\nu s$)	9.7×10^4 to 2.9×10^5	3.7×10^4 to 1.1×10^5	1.5×10^4 to 4.4×10^4
Approach Flow Reynolds Number ($R_a = u_a s_a/\nu$)	1.5×10^4 to 1.5×10^5	5×10^3 to 5×10^4	2×10^3 to 2×10^4
Weber Number ($W_d = \rho u^2 d/\sigma$)	1.1×10^4 to 3.2×10^4	2.0×10^3 to 8.0×10^3	6.0×10^2 to 2.0×10^3

In the definitions of these numbers,

- u = average velocity of flow in the pipe
- Q = flowrate in the pipe
- s = pipe submergence
- s_a = depth of approach flow at the containment floor
- u_a = average velocity of approach flow above containment floor
close to the sump floor depression
- ν = kinematic viscosity of water
- ρ = density of water
- σ = surface tension, water to air

4.1 Vortexing

4.1.1 Free-Surface Vortices

Free-surface vortices were identified as per the vortex type classification shown on Figure A3 in Appendix A. Average vortex type over a test is used as an indicator of vortex severity, and the stronger vortex was considered if more than one vortex was present. Figures 3 to 5 show the test average vortex types plotted against Froude number for each of the three test cases; namely, uniform approach flow, one pipe operation, and screen blockage tests, respectively. These figures indicate no trends with respect to scale effects on modeling free-surface vortices. Both models predicted the full scale test average vortices very well (mostly within ± 0.5 vortex type), except in the case of one pipe operation where both the 1:2 and 1:4 scale models indicated slightly higher vortex types than the full scale tests. Since any scale effects would give a reverse trend, this difference is ascribed to other but unknown reasons.

Figures 6a to 6c show the persistence of vortices observed during the tests using a plot of percentage of time the vortex is greater than or equal to type T versus the vortex type, T. All the tests for each of the three cases are included since Figures 3 to 5 showed no scale effects based on the average vortex type. Figure 6 addresses the distribution of vortex types during the tests. No scale effects in the persistence of various vortex types are apparent for any of the cases except for one pipe operation, where the model vortices are seen to be more persistent. This was also seen on Figure 4. The reason for this exception could be related to the relatively low turbulence levels at the very small model approach velocities.

To get an approximate idea of the circulation associated with an air-core (free-surface) vortex in the models and full scale sump at corresponding flow conditions, the angular velocity at the surface at a distance equal to the radius of the pipe from the vortex center was measured. This was accomplished by noting the average revolutions per minute of the floating device shown on Figure 7. A screen blockage test with $F = 0.5$ and $s/d = 2.5$ was selected for these tests as this condition provided a stable and persistent strong vortex, allowing convenient measurements. Table 5 shows that the full scale angular velocities are well predicted by the models based on Froude scaling.

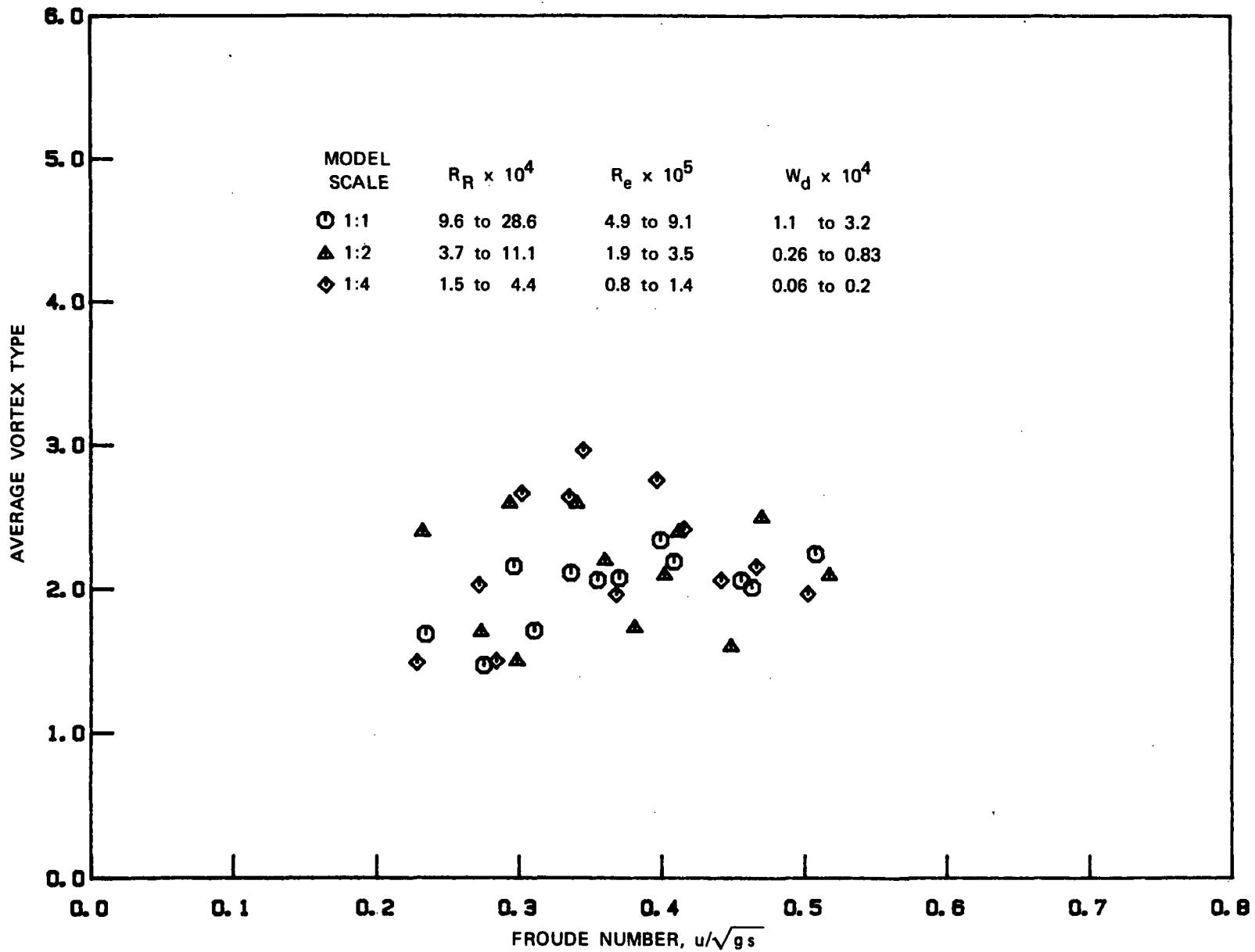


FIGURE 3 AVERAGE VORTEX TYPE DATA FOR UNIFORM APPROACH FLOW,
 BOTH PIPES OPERATING, TESTS

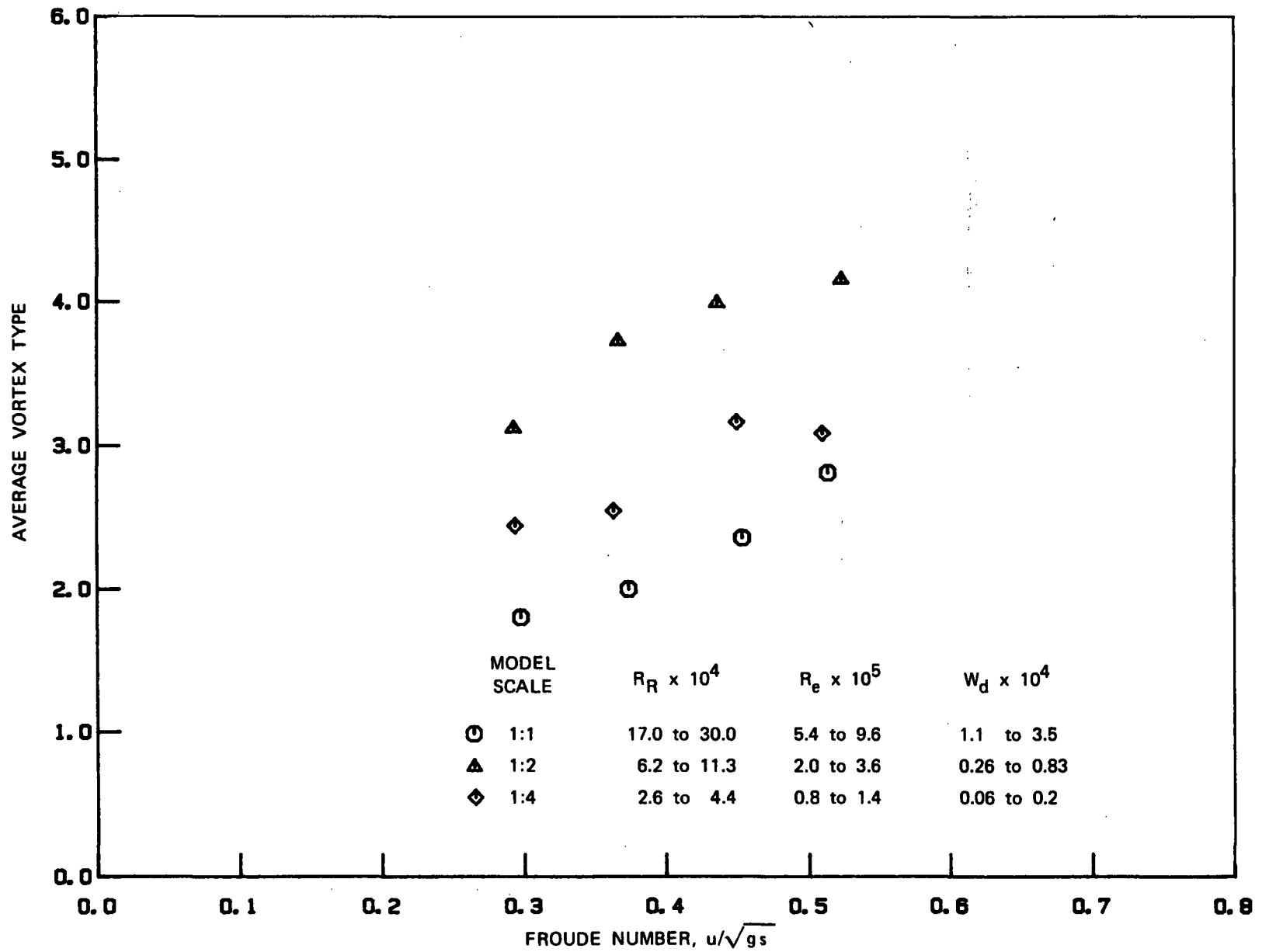


FIGURE 4 AVERAGE VORTEX TYPE DATA FOR ONE PIPE ONLY TESTS,
 $s/d = 2.5$

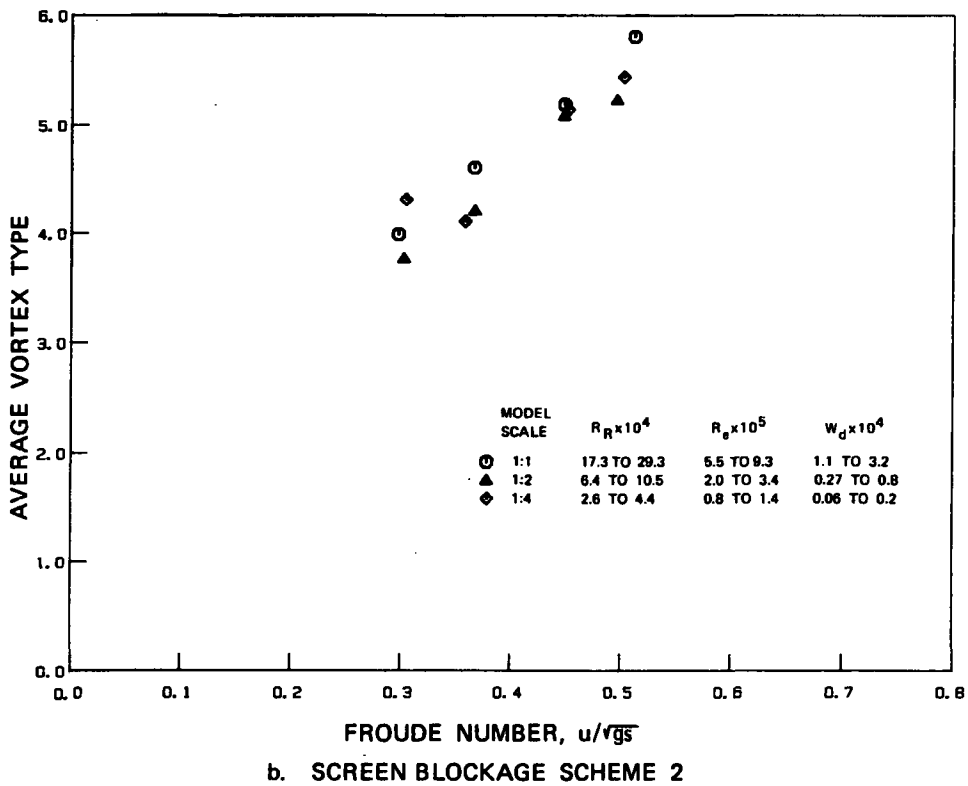
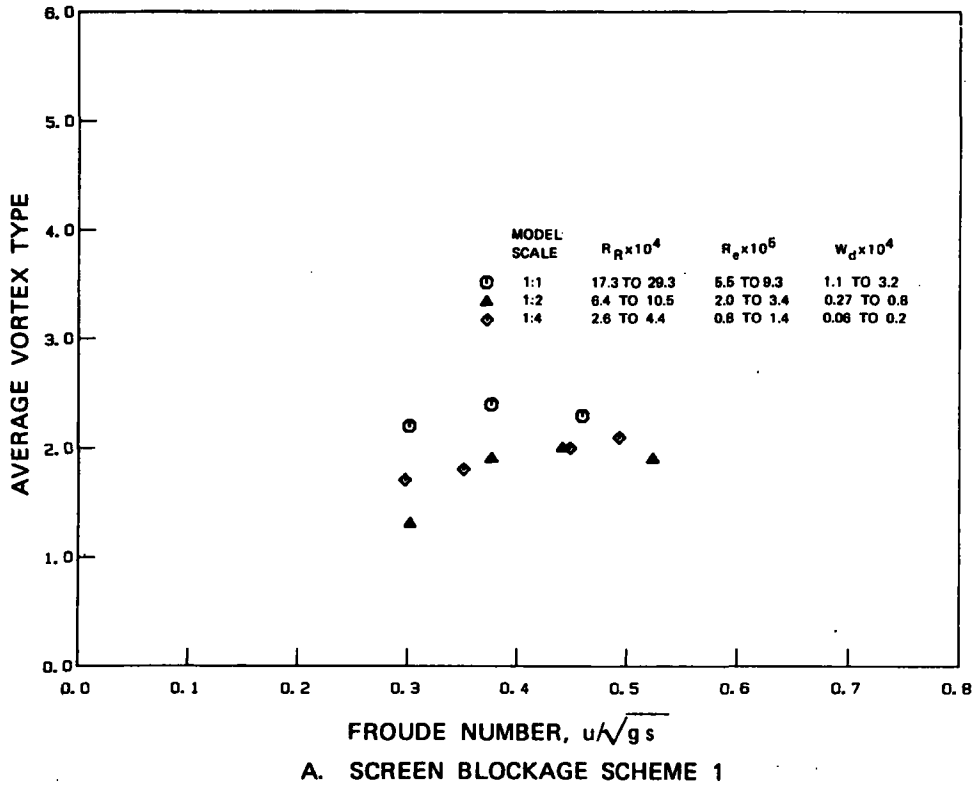
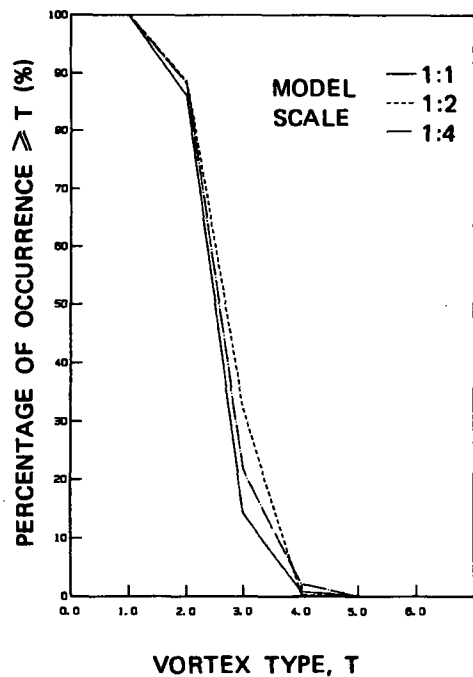
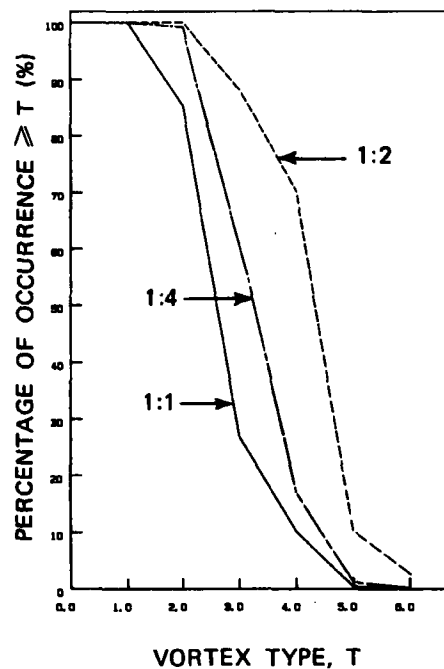


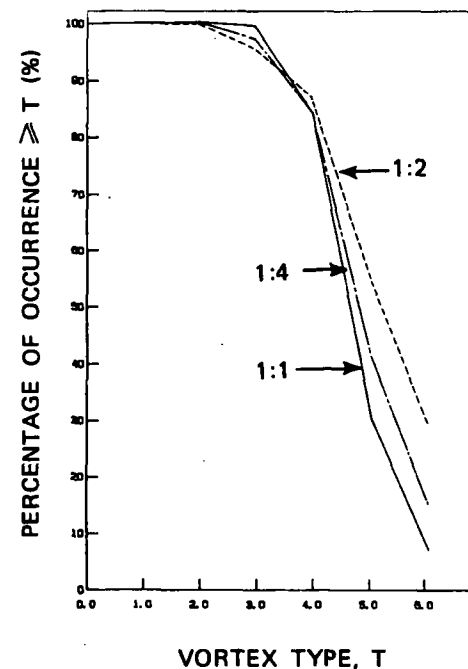
FIGURE 5 AVERAGE VORTEX TYPE DATA FOR SCREEN BLOCKAGE TESTS; $s/d = 2.5$; BOTH PIPES OPERATING.



A. UNIFORM APPROACH FLOW, BOTH PIPES OPERATING



B. ONE PIPE OPERATING, ALL TESTS WITH $s/d = 2.5$ CONSIDERED



C. SCREEN BLOCKAGE SCHEME 2; ALL TESTS AT $s/d = 2.5$ CONSIDERED

FIGURE 6 PERSISTENCE OF VORTICES FOR MODELS AND PROTOTYPE

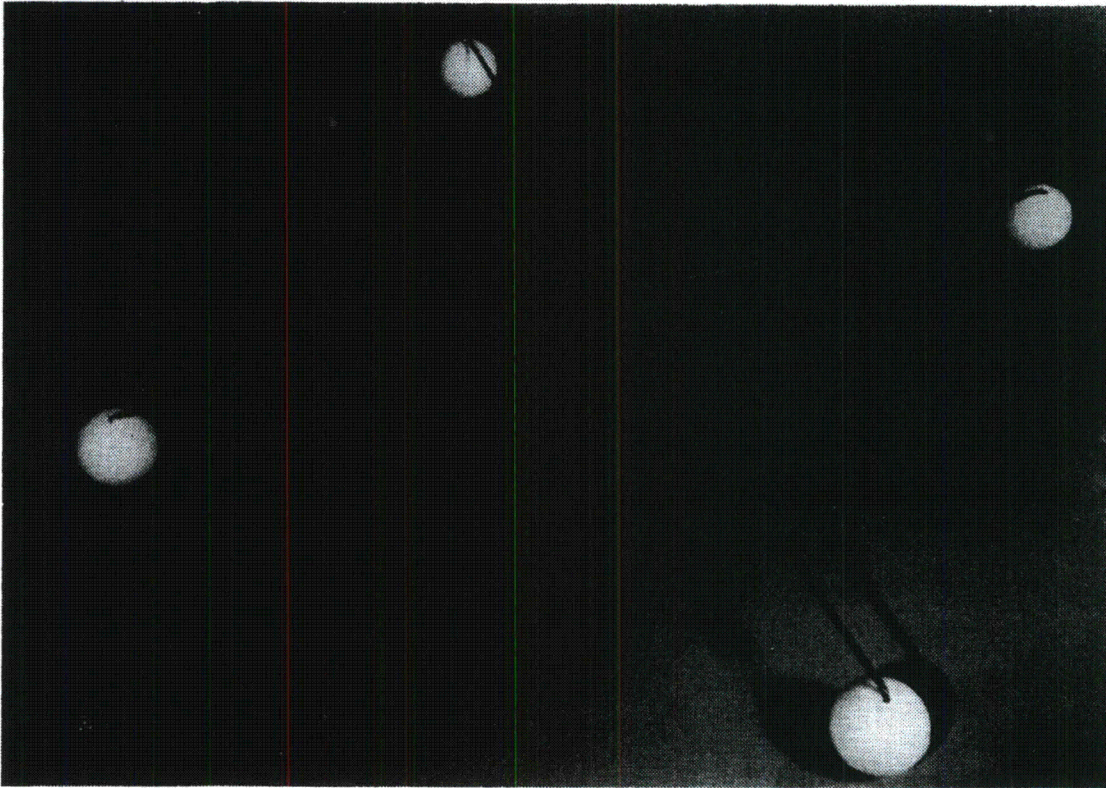


FIGURE 7 DEVICE FOR ANGULAR VELOCITY MEASUREMENT

TABLE 5
Measured Angular Velocities*

Model Scale	Froude Number	Radial	Pipe Reynolds Number x 10 ⁵	Measured	Froude** Scaled
		Reynolds Number x 10 ⁻⁵		ω_m rad/sec	ω_p rad/sec
1:4	0.5	0.4	1.4	1.85	0.93
1:2	0.5	1.1	3.4	1.33	0.94
1:1	0.5	2.9	9.3	1.03	1.03

*s/d = 2.5; with screen blockage scheme 2. Average of 10 readings of rpm used to calculate ω , measured at one pipe radius from vortex center.

** $\omega_p = \omega/t_r$ with $t_r = \sqrt{L_r}$; $t_r = 1/2$ for 1:4 and 1/1.414 for 1:2 model, where ω_m = model angular velocity; ω_p = full scale angular velocity.

The diameter of the surface depression for stable air-core vortices under comparable operating conditions was measured using photographs for the models and full scale sump. It was observed that the model vortex surface dimensions approximately corresponded to the geometric scales compared to the full size vortex dimensions.

To illustrate any Reynolds number effects on modeling vortexing, the average vortex type is plotted against the radial Reynolds number in Figure 8, for the uniform approach flow case. The pipe Reynolds number and Weber number ranges are noted in Figure 8. It may be concluded that within the tested ranges ($R_R > 1.5 \times 10^4$, $Re > 7.7 \times 10^4$ and $W_d > 600$), no viscous or surface tension scale effects on modeling free surface vortexing were noted. This finding supports those of Daggett and Keulegan (10) that viscous effects on vortices are negligible for $Re > 3 \times 10^4$ and to some extent, those of Jain et al (12) showing that for $W_d > 120$, no surface tension effects were found. Anwar et al (11) have prescribed a value for R_R greater than 3×10^4 for Reynolds number independence, and the present study, based on average vortex type, showed no R_R dependence with R_R equal to or greater than 1.5×10^4 . The definition of R_R as $Q/\nu s$ may not be appropriate for depressed floor sumps where s , the submergence, is not indicative of the approach flow conditions to the outlet. If the depth of approach flow, s_a , is used instead of s , and a Radial Reynolds number R_{Ra} is defined as $Q/\nu s_a$, the value of R_{Ra} in the present study would be above 2.5×10^4 .

4.1.2 Sub-Surface Vortices

For the uniform approach flow with both pipes operating, sub-surface vortices were observed extending from the front and back sump walls to each pipe. These vortices did not cause any air-entrainment, but appeared to affect the pipe flow swirl levels. The vortices were visible on dye injection and were intermittent and varying in strength. Figure 9 shows

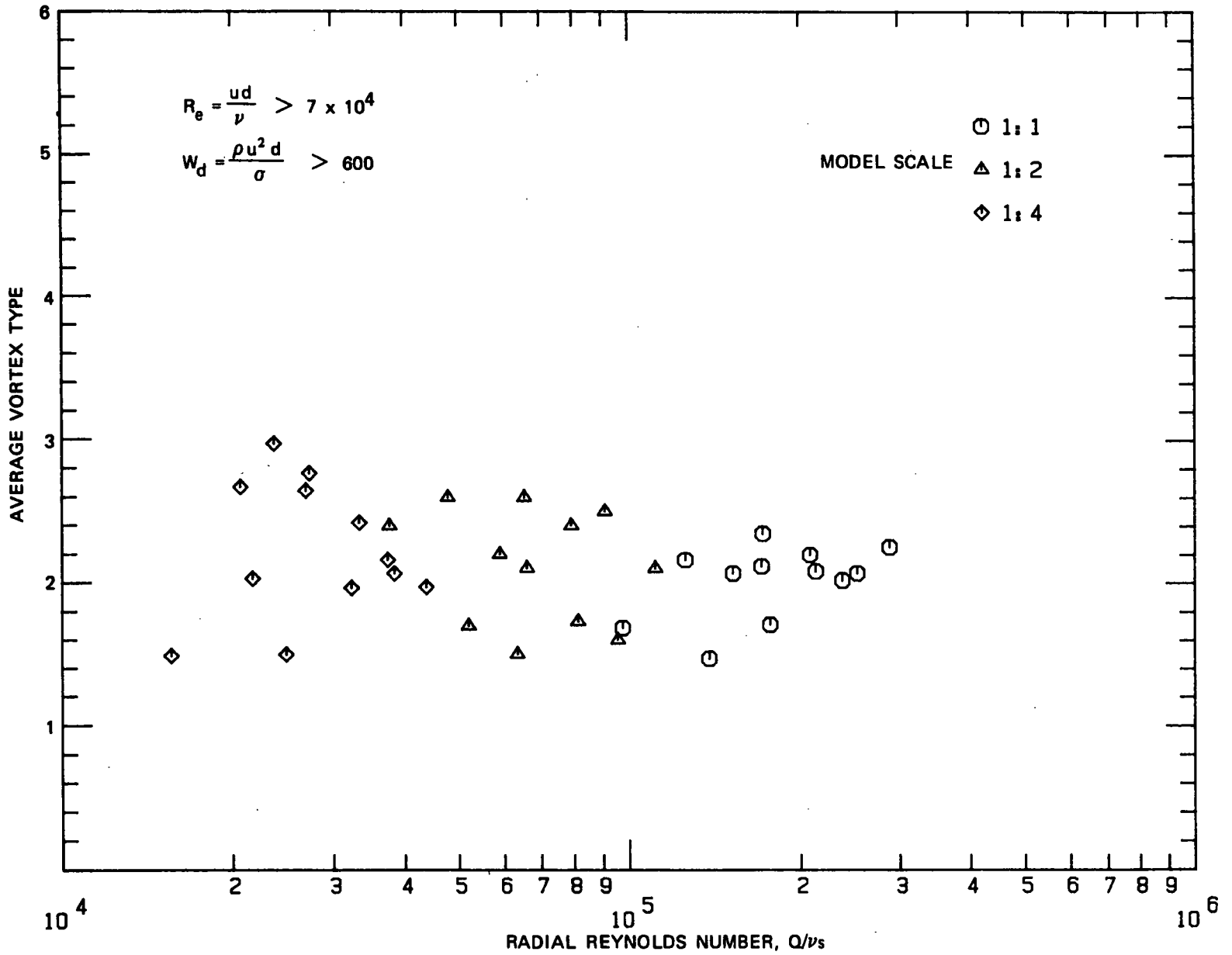
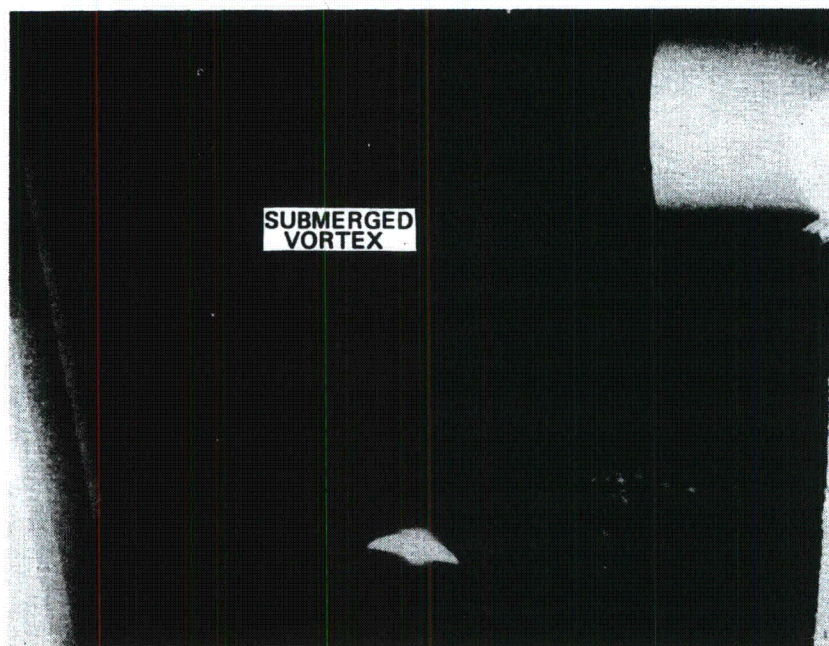
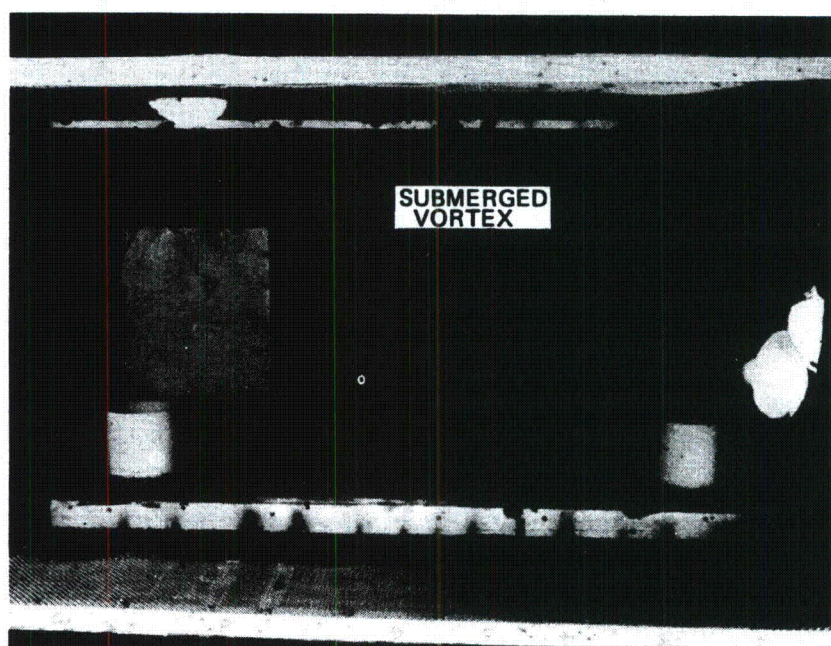


**FIGURE 8 AVERAGE VORTEX TYPES FOR VARIOUS RADIAL REYNOLDS NUMBERS;
 UNIFORM APPROACH FLOW; BOTH PIPES OPERATING**



a. 1:2 MODEL



b. 1:4 MODEL

FIGURE 9 TYPICAL SUB-SURFACE VORTICES (SUBMERGED VORTICES) IN SCALE MODELS; UNIFORM APPROACH FLOW; BOTH PIPES OPERATING; $s/d = 3$, $F = 0.47$, $d = 12''$ FOR 1:2 AND 6'' FOR 1:4 MODEL

photographs of the sub-surface vortex at the back wall in 1:2 and 1:4 models. The back wall vortex was more stable and stronger than the front wall vortex. The sub-surface vortices were visible but not very well organized in the 1:1 sump compared to the models, and it was difficult to photograph them. Also, these vortices were not well organized for screen blockage cases and one pipe operation cases for both the models and the 1:1 sump. The sub-surface vortices were found to result from the eddies at the shear layer generated as the flow entered the depressed sump from the front, back and sides of the sump. They were found to induce considerable swirl in the pipes since the swirl meter indicated higher swirl angles at lower submergences when the sub-surface vortices were stronger and free-surface vortexing was not significant. The strength of sub-surface vortices was not measurable directly, however, the swirl meter readings could be considered to indicate the influence of these vortices.

4.2 Air-Withdrawals Due to Vortices

The selected 1:1 sump was operated in a Froude number range of about 0.23 to 0.51, and higher Froude numbers could not be achieved since the maximum possible flow with both pipes operating was limited to about 9000 gpm/pipe. Depths of approach flow upstream of screens was limited to about 2 ft to avoid excessively small depths in reduced scale models. No air-core vortices were observed for cases without screen blockages. Even though intermittent air-core vortices were observed for tests with screen blockages for the tested Froude number range, these vortices were weak in terms of air-withdrawals and produced less than 0.2% maximum 1 minute average void fraction at the measurement location (about 1 psig). Since these void fractions are very low, within the accuracy range of the void fraction meter, only an overall comparison of the void fraction values with those obtained from the reduced scale models at comparable operating conditions can be made. Figure 10 shows the void fraction versus Froude number plots for the 1:1, 1:2, and 1:4 scaled tests for screen blockage scheme 2 (for scheme 1, void fraction data were not obtained since vortices were even weaker). It may be concluded that within the accuracy of measurements, both the 1:2 and 1:4 models operated with Froude law predicted air-withdrawals in terms of void fractions closely and, as such, no scale effects were apparent. This is in conformance with the fact that the vortex core sizes appeared to be simulated to scale in the models, as previously discussed.

5.3 Pipe Swirl

Intensities of swirl in the suction pipes were calculated in terms of indicated swirl angles using the swirl meter readings. The swirl angle, θ , is given by

$$\theta = \tan^{-1} \left(\frac{\pi n d}{u} \right) \quad (10)$$

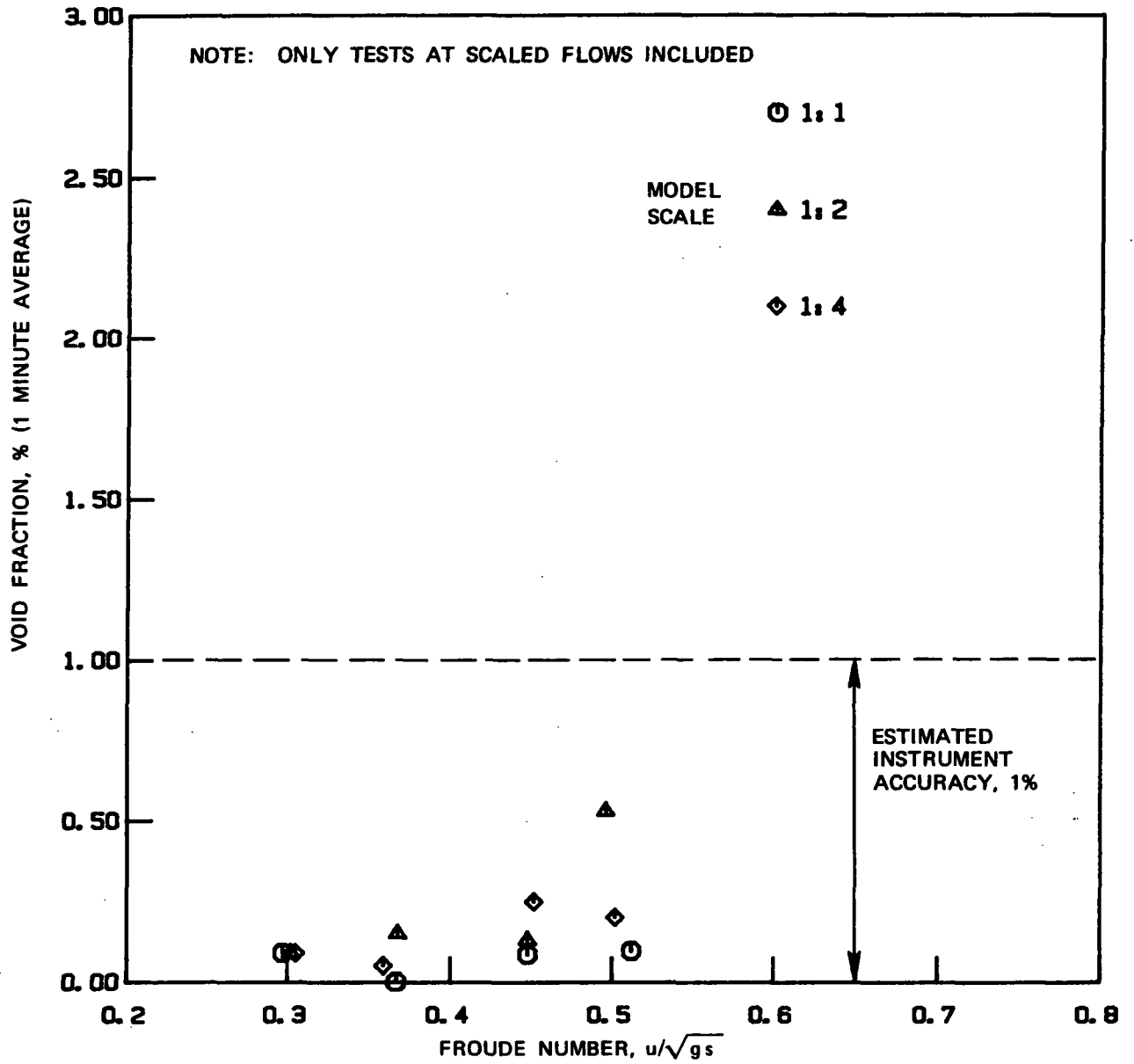


FIGURE 10 AIR-WITHDRAWALS DUE TO AIR-CORE VORTICES FOR THE SCALE MODELS TESTED WITH SCREEN BLOCKAGE SCHEME 2 ; $s/d=2.5$

where

n = number of revolutions/sec of swirl meter
 d = pipe internal diameter, ft
 u = average axial velocity, ft/sec

The measurement location of swirl was about 8 pipe diameters from the inlet for 1:1 and 1:4 scale sumps, while for 1:2 sump, it was 11 pipe diameters. Hence, a correction to the swirl readings accounting for the swirl decay over the extra three pipe diameters was made for the 1:2 sump so as to get an equivalent value of swirl angles at 8 pipe diameters. A correction factor was determined based on available literature on pipe swirl decay following an exponential law (16, 17),

$$\frac{\tan \theta_1}{\tan \theta_2} = e^{\beta \Delta x/d} \quad (11)$$

where

θ_1 = swirl angle at distance x from inlet
 θ_2 = swirl angle at distance x + x from inlet
 β = a decay factor

Assuming an average pipe Reynolds number of 2.5×10^5 and a swirl level of about 20 degrees at x, a constant value of $\beta = 0.06$ was used, resulting in a correction factor of about 1.2 (16).

The pipe swirl could be generated due to both the free-surface and sub-surface vortices and also could be affected by the flow pattern at the pipe entrance. For uniform approach flow tests, it was found that sub-surface vortices had the major influence on pipe swirl. The free-surface vortices were weak in this case and sub-surface vortices were observed to be stronger for lower submergences, causing higher swirl angles. Figures 11 to 13 show the swirl angles to Froude number relationship for various submergences for the 1:1 scale, 1:2 scale, and 1:4 scale sumps, respectively, all for the uniform approach flow with both pipes operating. It can be seen that swirl is dependent on pipe submergence, which could be due to the observed dependence of sub-surface vortices to submergence at a given Froude number. The 1:4 model shows a significant increase in swirl with Froude number for a given submergence, which is not the case with 1:1 and 1:2 models. This may be due to some Reynolds number effects on the swirl in the 1:4 model, as discussed in later paragraphs.

Figures 14 and 15 show the swirl angles to Froude number relationship for a submergence ratio s/d of 2.5 for the 1:1, 1:2, and 1:4 scale sumps for one pipe operation and screen blockage (schemes 1 and 2). Both the reduced scale models show increasing swirl with increasing Froude number for both one pipe operation and screen blockage. As the free surface vortices were not a strong function of Froude number over the tested range, perhaps there exists some Reynolds number effect on swirl due to sub-surface vortices which are related to pipe swirl. This aspect is further investigated below.

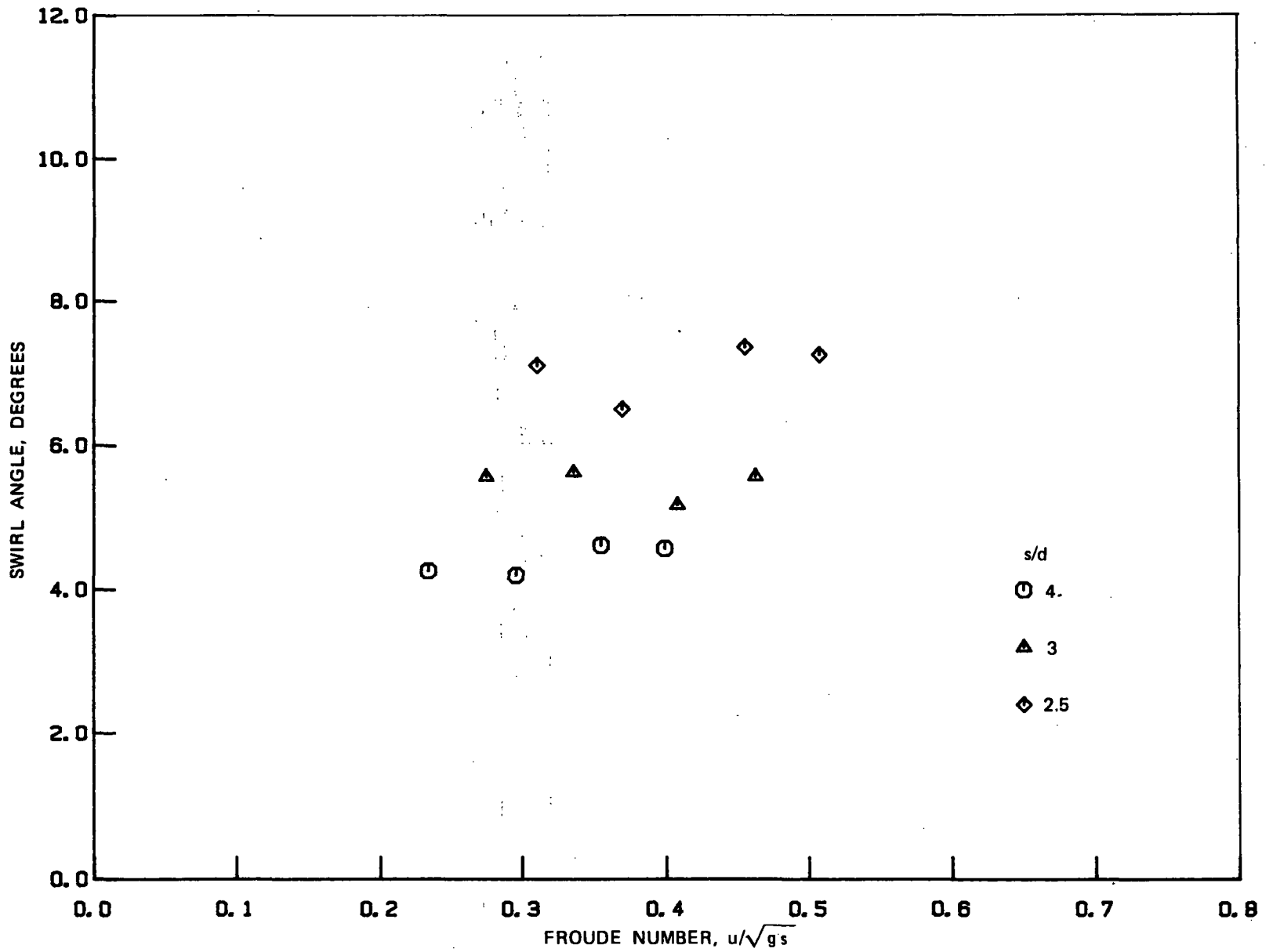


FIGURE 11 SWIRL ANGLE DATA FOR VARIOUS SUBMERCENCES; 1:1 SCALE MODEL; UNIFORM APPROACH FLOW; BOTH PIPES OPERATING

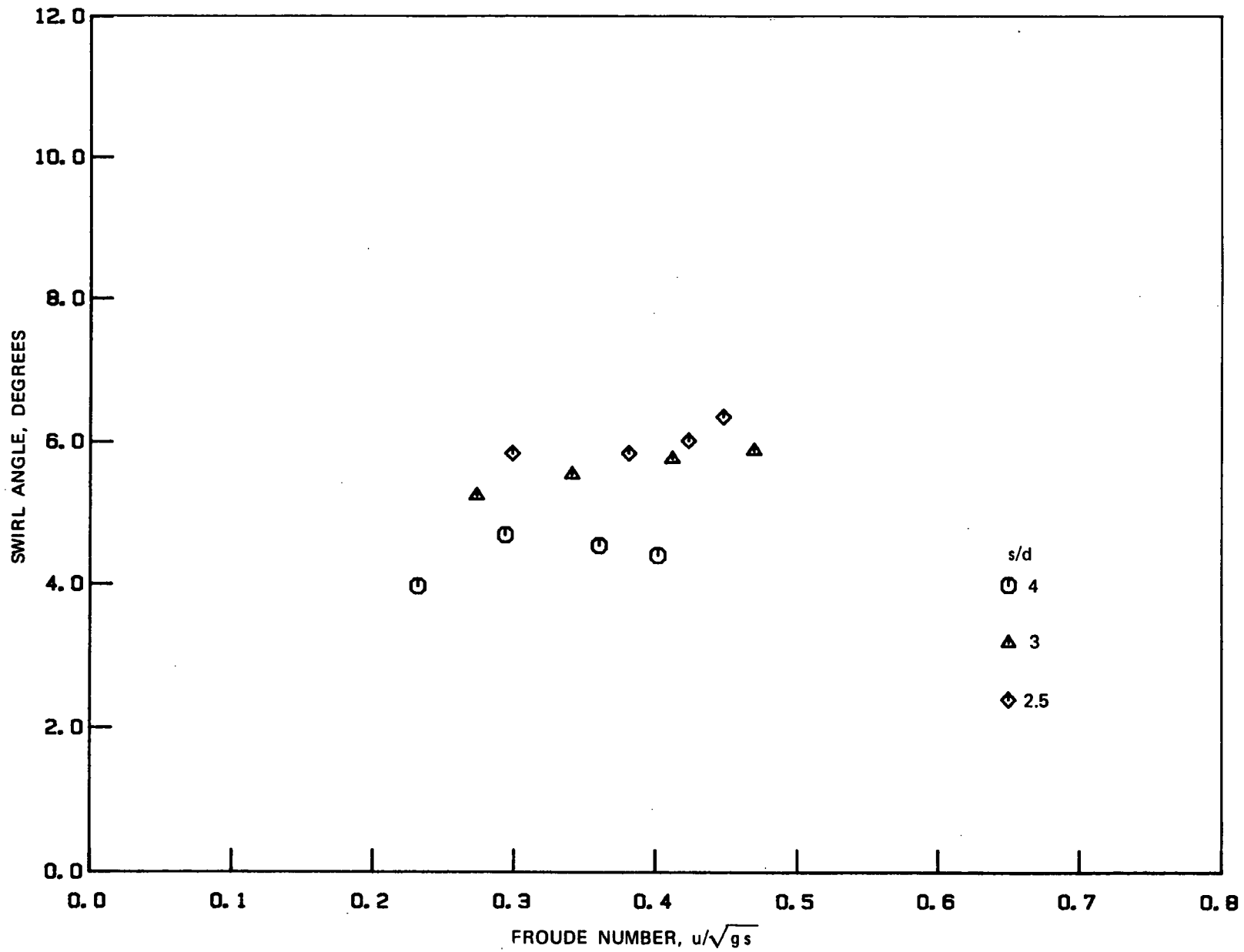


FIGURE 12 SWIRL ANGLE DATA FOR VARIOUS SUBMERGENCES; 1:2 SCALE MODEL; UNIFORM APPROACH FLOW; BOTH PIPES OPERATING

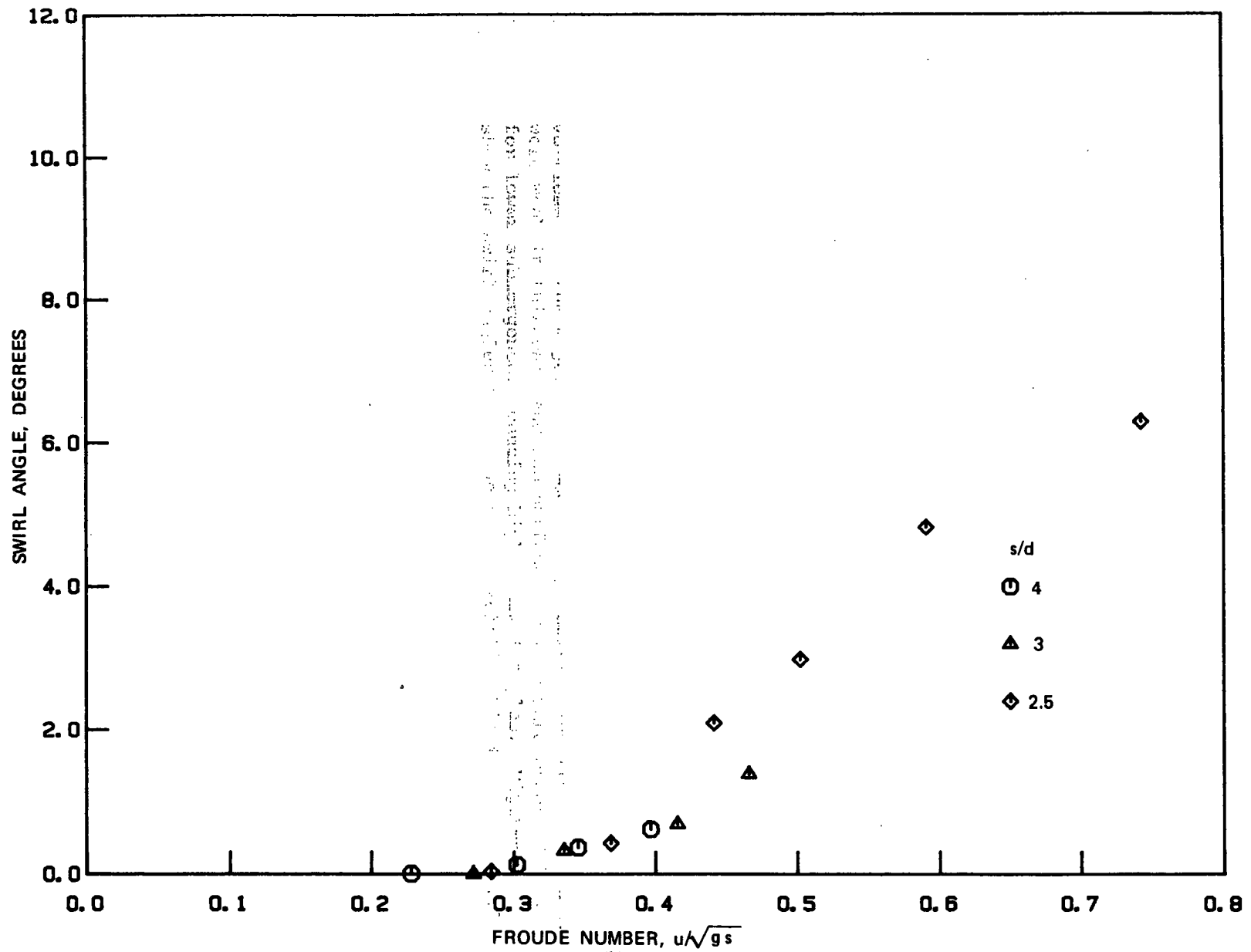


FIGURE 13 SWIRL ANGLE DATA FOR VARIOUS SUBMERCENCES; 1:4 SCALE MODEL; UNIFORM APPROACH FLOW; BOTH PIPES OPERATING

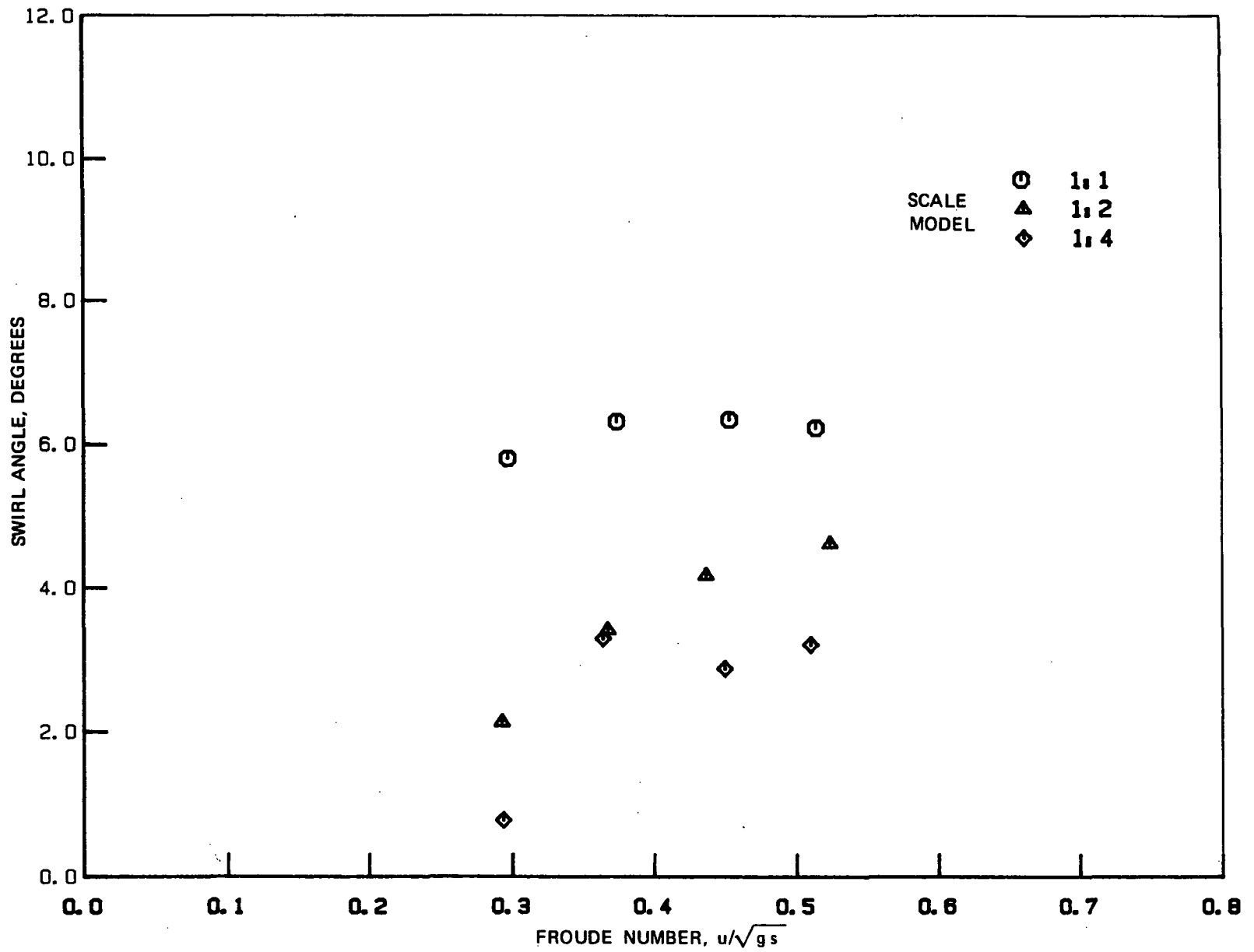
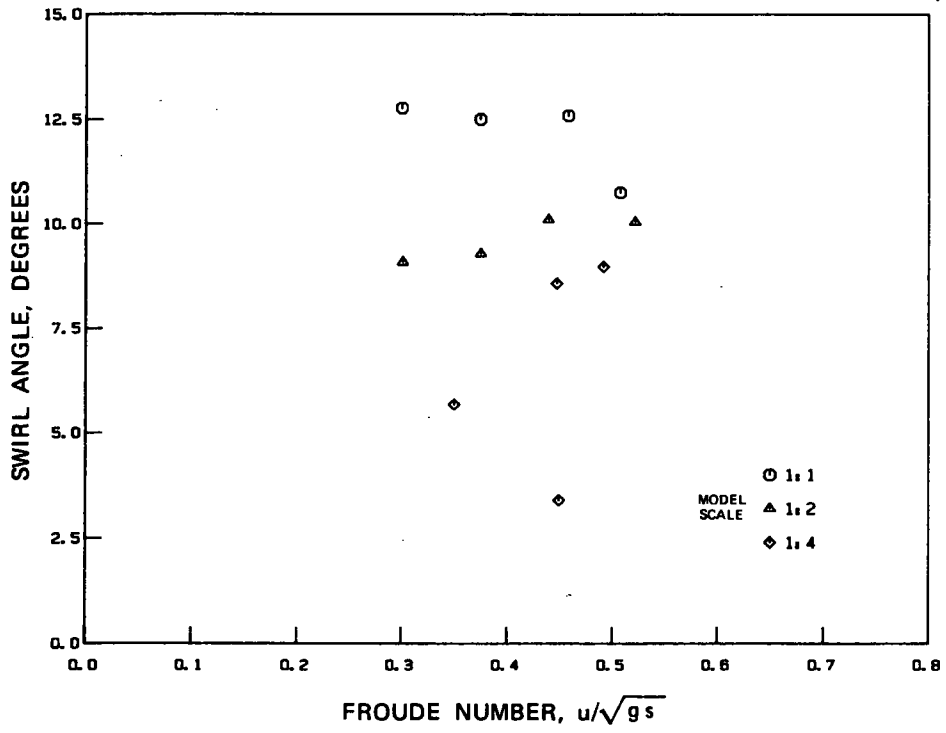
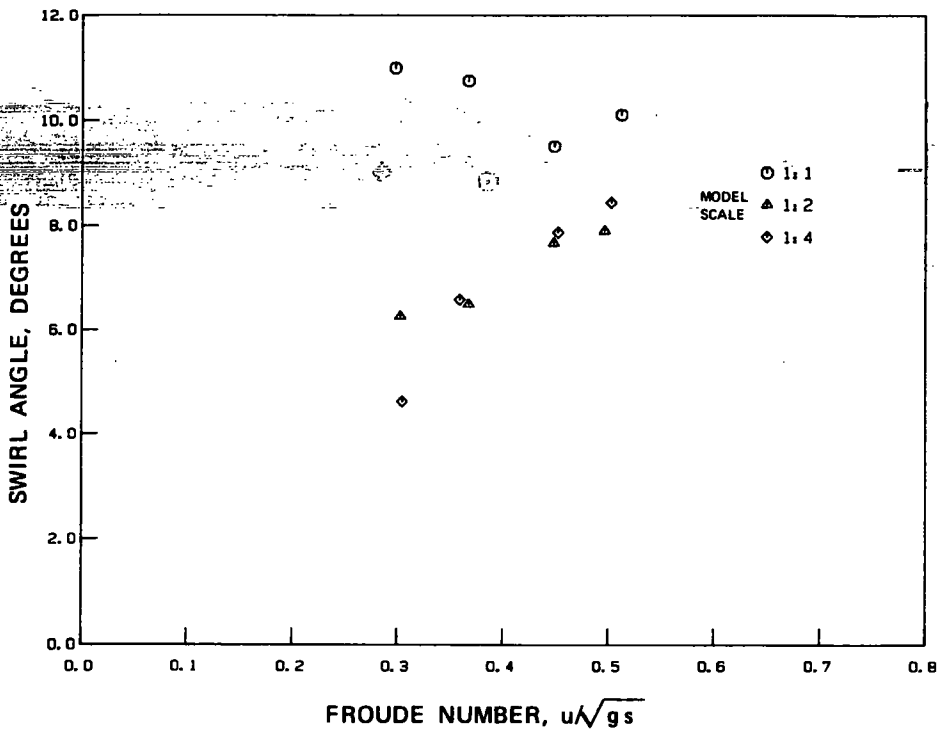


FIGURE 14 SWIRL ANGLE VERSUS FROUDE NUMBER; ONE PIPE OPERATING;
 $s/d = 2.5$



a. SCREEN BLOCKAGE SCHEME 1



b. SCREEN BLOCKAGE SCHEME 2

FIGURE 15 SWIRL ANGLE VARIATION WITH FROUDE NUMBER; SCREEN BLOCKAGES; PIPE 2 DATA; $s/d = 2.5$

As described in Section 5.1.2, sub-surface vortexing resulted from the shear layer generated at the floor depression, and these vortex filaments contributed to the measured swirl in the pipes. Since the velocity gradient across the shear layer is a function of the approach velocity at the floor depression, it is considered appropriate to use an approach flow Reynolds number when examining any Reynolds number effects on the swirl in the pipes. The radial Reynolds number, $R_R = Q/vs$, defined by Anwar *et al* (11), is a representative approach flow Reynolds number for a single suction outlet with no depressed floor sump. However, the existence of a depressed floor (sump floor below containment floor) and consideration of screen blockage, makes the use of R_R (defined using a single pipe flow and submergence) inappropriate when considering the swirl due to: (a) an approach flow depth much smaller than the pipe submergence(s); (b) the flow in a given pipe which is less than the total approach flow with two pipes operating; and (c) for screen blockage cases where, the approach flow velocity depends on the unblocked area of the screens.

For the present study, a new approach flow Reynolds number, R_a , is defined as,

$$R_a = \frac{u_a s_a}{\nu}$$

where

u_a = average approach velocity above the containment floor at the sump floor depression (see Figure 1)

s_a = approach flow depth above the containment floor at the sump (see Figure 1)

Figures 16 to 18 show plots of θ/θ_a versus approach flow Reynolds number, R_a , for uniform approach flow (both pipes operating), one pipe operating, and screen blockage (scheme 2), respectively. θ is the measured swirl angle for the reduced scale models, while θ_a is the average measured swirl angle for the 1:1 scale sump. For the 1:1 sump, θ/θ_a is close to one, allowing for experimental scatter, which appears to be about $\pm 10\%$. For the 1:2 and 1:4 models, any significant deviations (above a possible scatter of $\pm 10\%$) from the value of 1.0 for θ/θ_a can be considered as denoting possible scale effects due to lower R_a values in the reduced scale models. In Figures 16 to 18, the data for submergence corresponding $s/d = 2.5$ are used since the desired data are available for all of the cases at this submergence, making a wide range of R_a possible.

In Figure 19, all the data points of Figures 16 to 18 are collapsed on a single plot and an average curve is fitted. It can be seen from these figures that above a value of $R_a \approx 3 \times 10^4$, the models do predict the swirl angles within $\pm 10\%$ of the average values in the full scale sump.

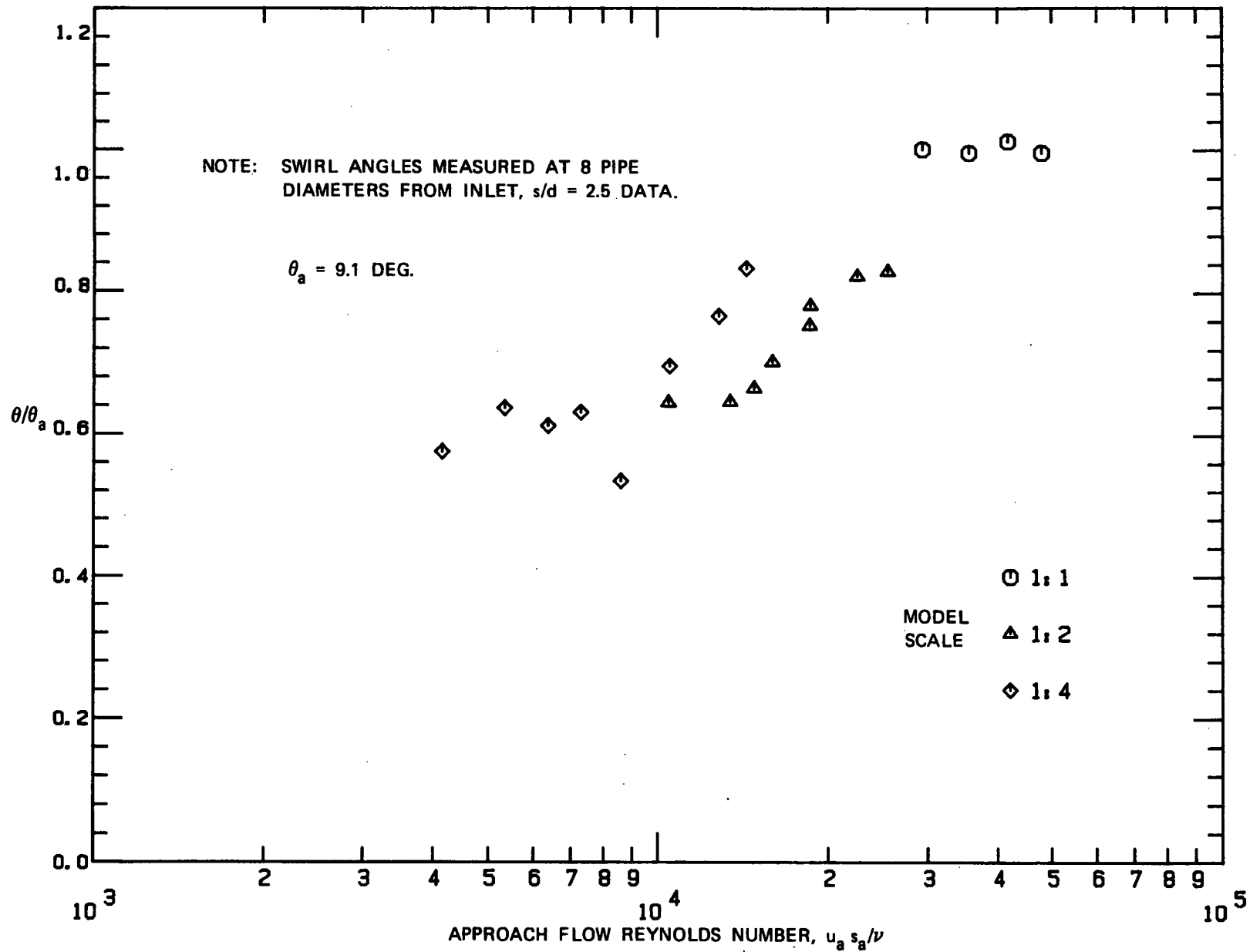


FIGURE 16 VARIATION OF RATIO OF MEASURED SWIRL ANGLES TO AVERAGE PROTOTYPE MEASURED SWIRL ANGLE WITH APPROACH FLOW REYNOLDS NUMBER, UNIFORM APPROACH FLOW, BOTH PIPES OPERATING

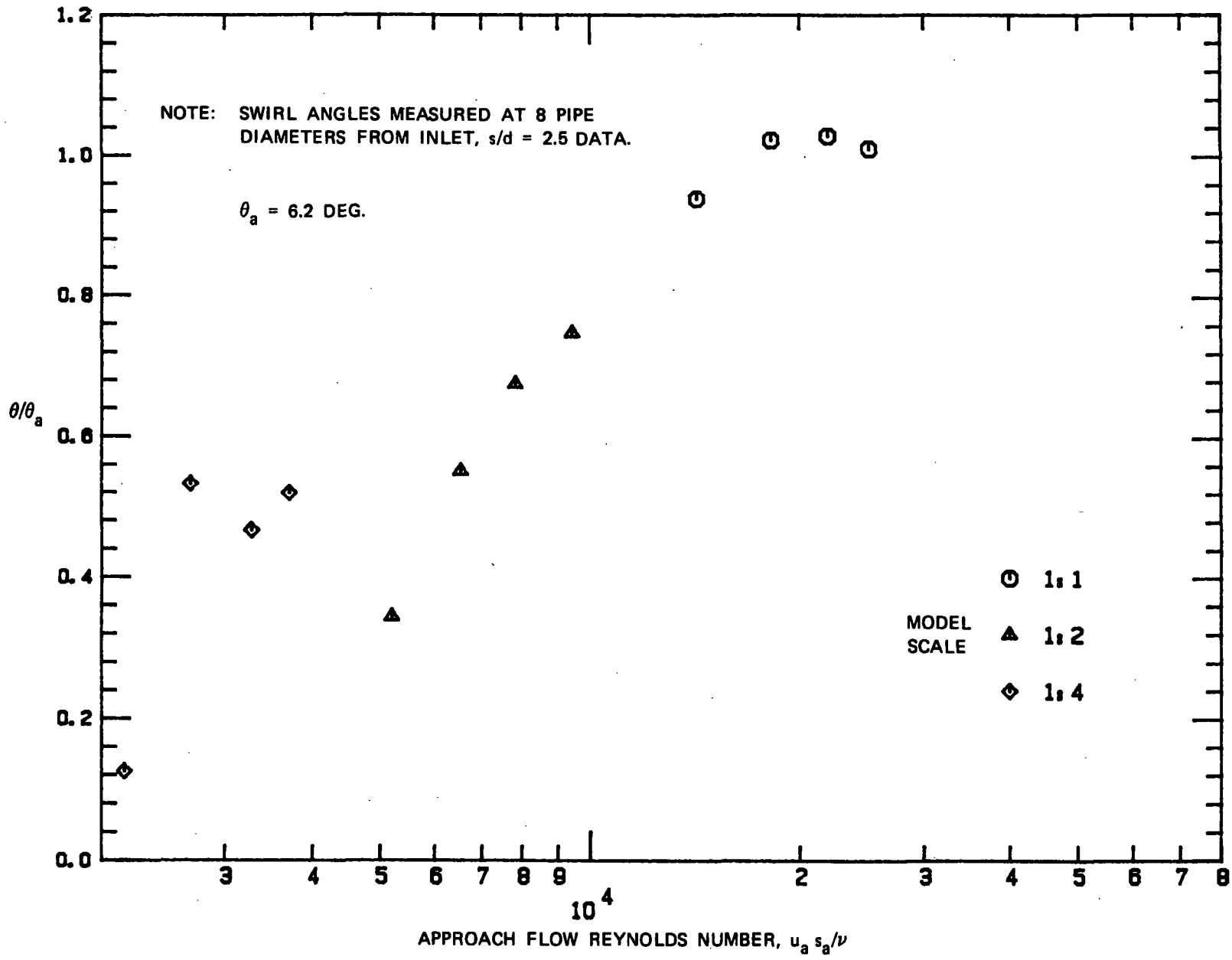


FIGURE 17 VARIATION OF RATIO OF MEASURED SWIRL ANGLES TO AVERAGE PROTOTYPE MEASURED SWIRL ANGLE WITH APPROACH FLOW REYNOLDS NUMBER, ONE PIPE OPERATING

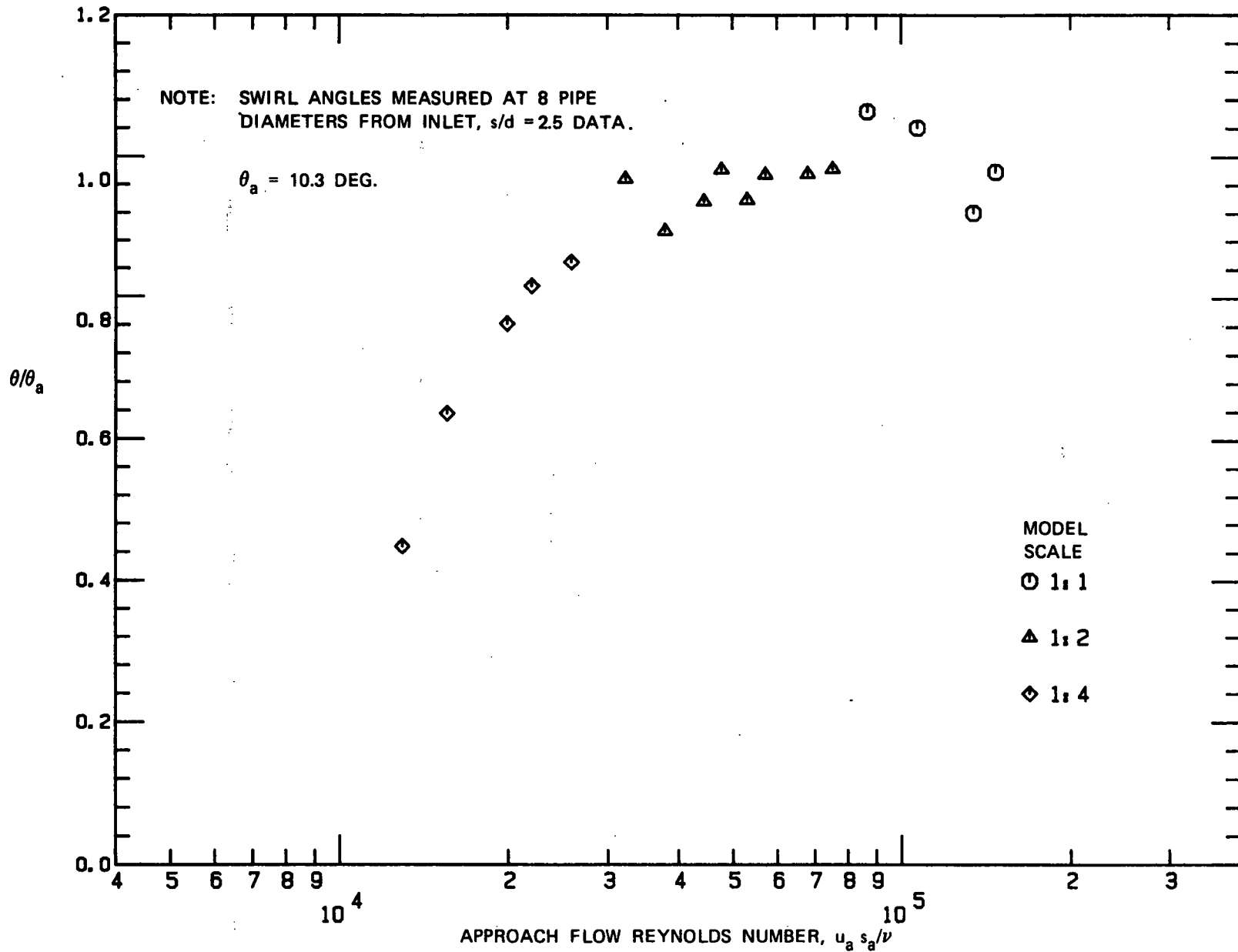


FIGURE 18 VARIATION OF RATIO OF MEASURED SWIRL ANGLES TO AVERAGE PROTOTYPE MEASURED SWIRL ANGLE WITH APPROACH FLOW REYNOLDS NUMBER, SCREEN BLOCKAGE SCHEME 2

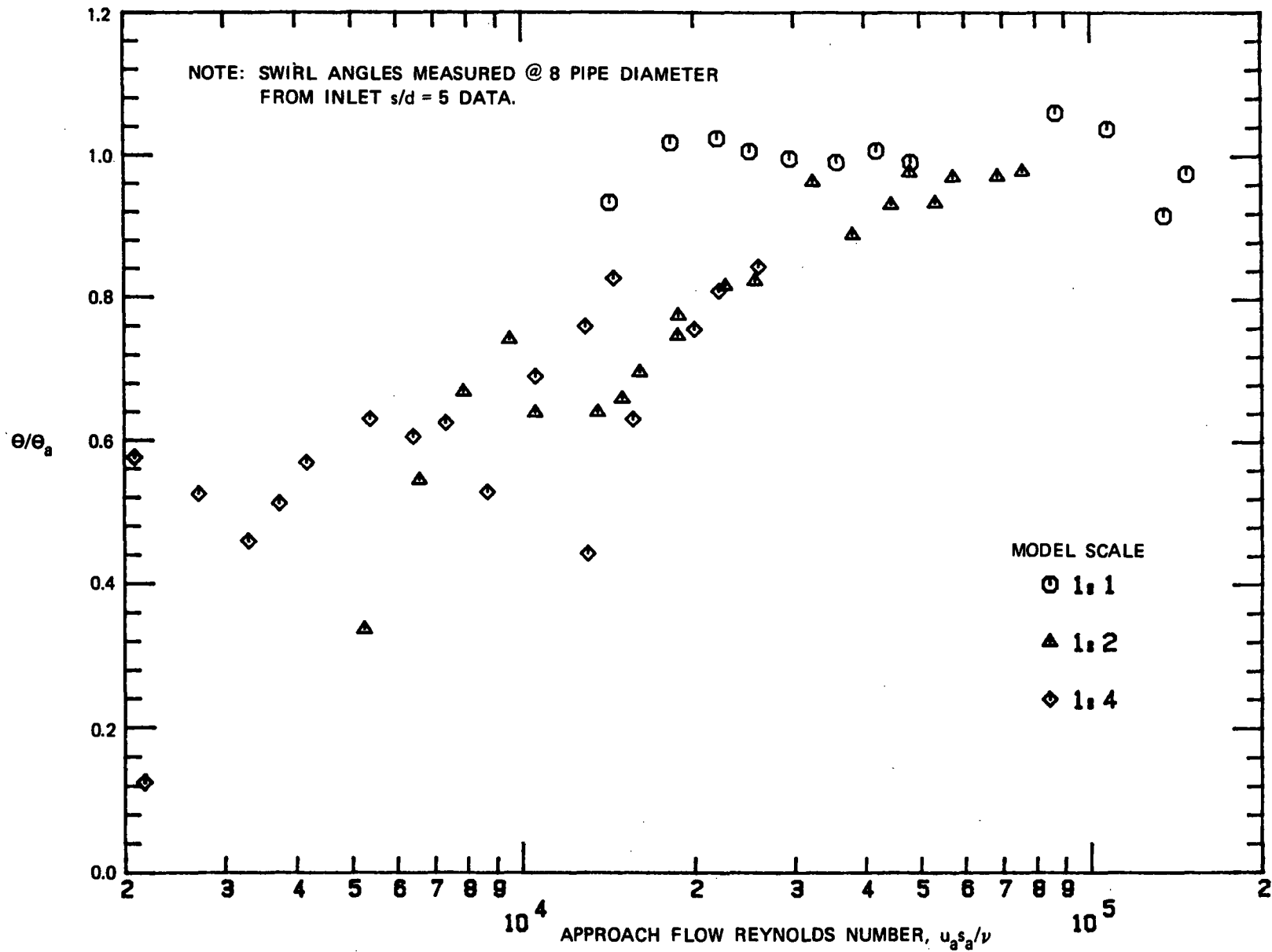


FIGURE 19 VARIATION OF RATIO OF MEASURED SWIRL ANGLES TO AVERAGE PROTOTYPE MEASURED SWIRL ANGLE WITH APPROACH FLOW REYNOLDS NUMBER; ALL DATA FOR $s/d = 2.5$ INCLUDED.

Since available literature on swirling pipe flow (16, 17) indicate that the swirl decay rate along the pipe length is a function of pipe Reynolds number R_e , decreasing with increasing R_e , the effect of the reduced ranges of R_e in the scaled models could have contributed towards a lower measured swirl compared to the full size sump. Using the empirical relationship given in (17), $\beta = K(R_e^{0.7})$, where K is a constant, the swirl angles at 2 pipe diameters from the inlet were calculated. This removed the influence of R_e on the measured pipe flow swirl downstream of the inlet, and allows evaluation of the flow swirl close to the pipe inlet. Figure 20 shows $\theta_i/(\theta_i)_a$, the ratios of the calculated inlet swirl at 2 pipe diameters from the entrance in the reduced scale model to the average inlet swirl at 2 pipe diameters from the pipe entrance in the full sized sump. These calculations show there is an approach flow Reynolds number R_e affect on flow swirl angles, even after accounting for pipe R_e affects in pipe swirl decay. Viscous scale effects on inlet swirl, contributing to underprediction of swirl in the reduced scale models, were noticed in the tests at both Froude scaled flows and prototype velocities reported by Reddy and Pickford (18). Their experiments involved vertical suction pump inlets and showed no free-surface vortexing, but indicated swirl at the inlet, presumably due to flow patterns at the entrance of the pipe and sub-surface vortices.

Considering the above results, reduced scale models of sumps with a floor depression should have an approach flow Reynolds number equal to at least 3×10^4 for a correct prediction of flow swirl angles. If such values of R_e cannot be achieved by Froude scaled flows, tests may be conducted at higher than Froude velocities, keeping the submergence constant, so as to obtain a better prediction of flow swirl in the inlet pipe.

4.4 Inlet Losses

The method of evaluating inlet losses, including screen and grating losses from pressure gradient measurements, is explained in Section 3.0. Figure 21 shows the loss coefficient, C_L , plotted against Froude number for a submergence ratio $s/d = 4, 3, \text{ and } 2.5$, for the 1:1, 1:2, and 1:4 sumps with uniform flow (both pipes operating). Within an estimated average data scatter of about ± 0.1 due to uncertainties associated with pressure measurements and method of evaluation, the loss coefficient is seen to be more or less independent of Froude number except for the 1:4 model, where slightly higher values of C_L are observed for lower Froude numbers. This may be partly due to lower accuracies of loss coefficient evaluation for smaller flows and/or perhaps also due to a possible Reynolds number dependence, as indicated in Figure 22. This figure shows that the loss coefficient

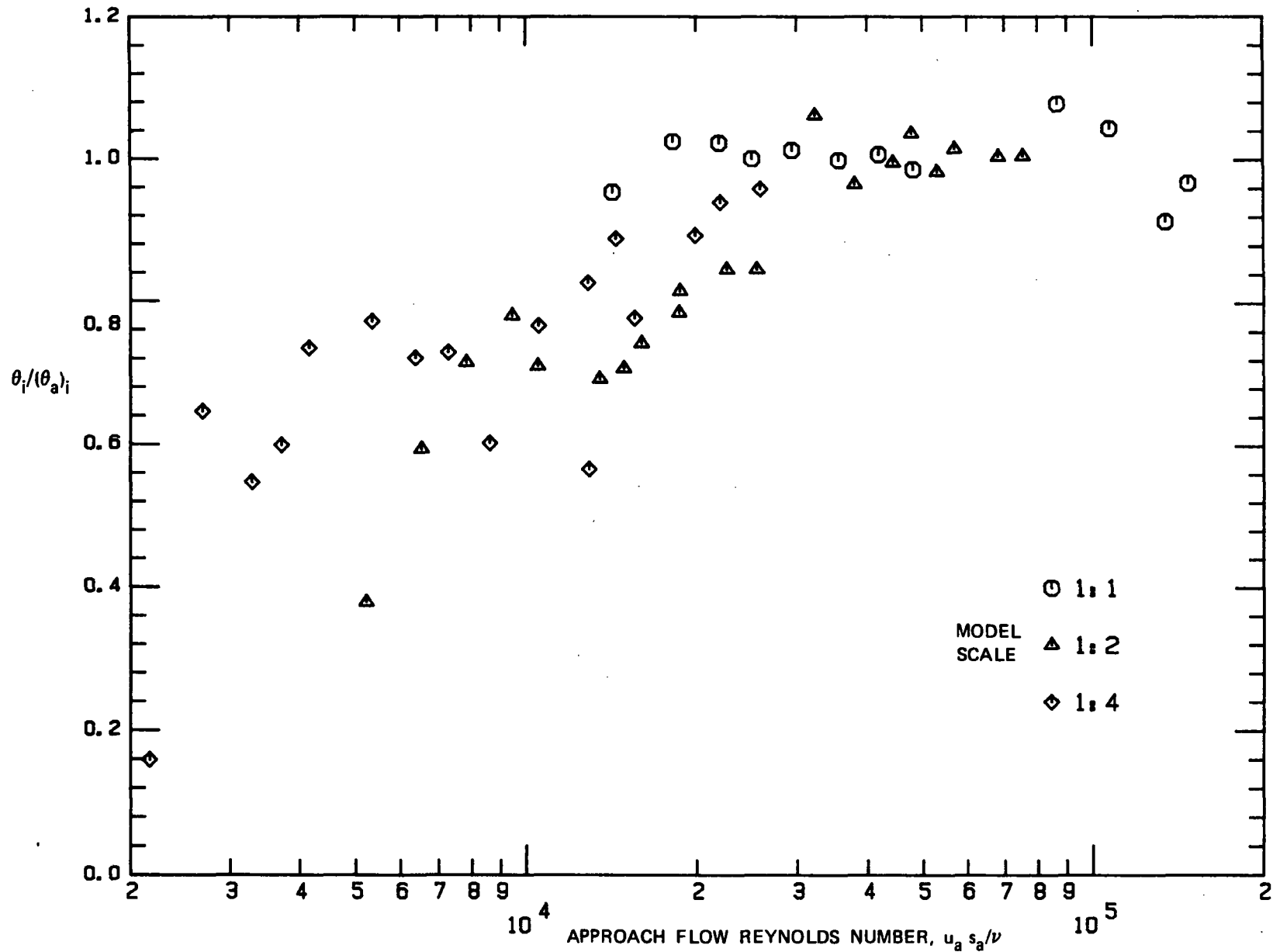


FIGURE 20 VARIATION OF THE RATIO OF SWIRL ANGLES NEAR INLET TO AVERAGE PROTOTYPE SWIRL ANGLE NEAR INLET WITH APPROACH FLOW REYNOLDS NUMBER; ALL DATA FOR $s/d = 2.5$

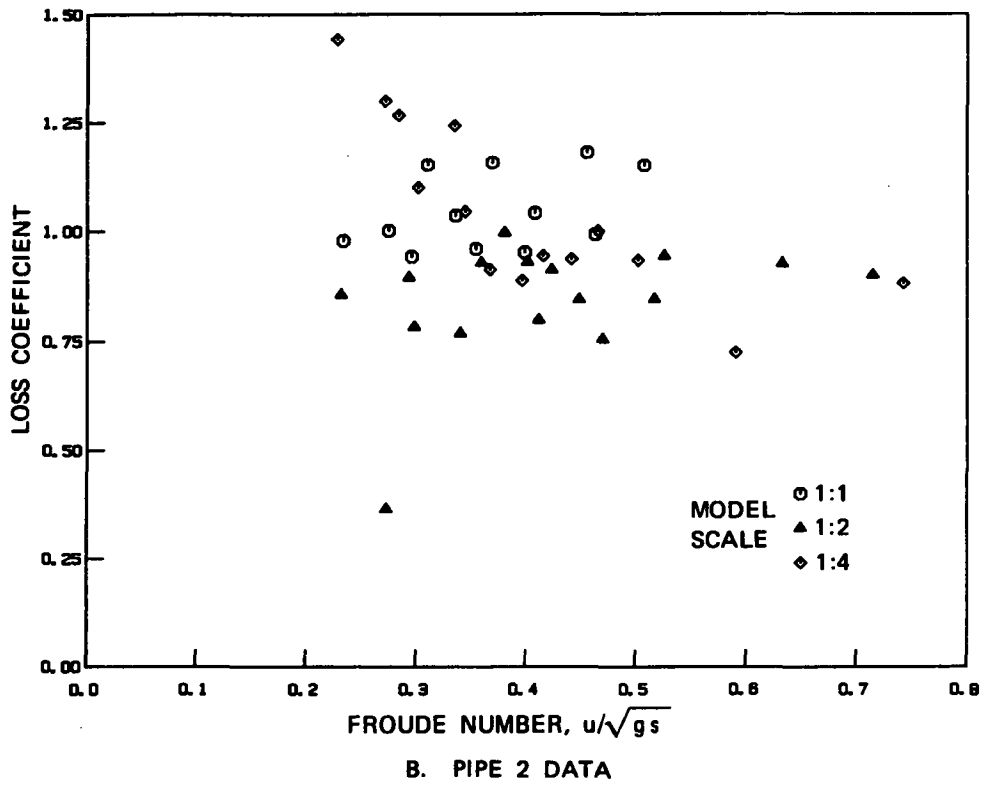
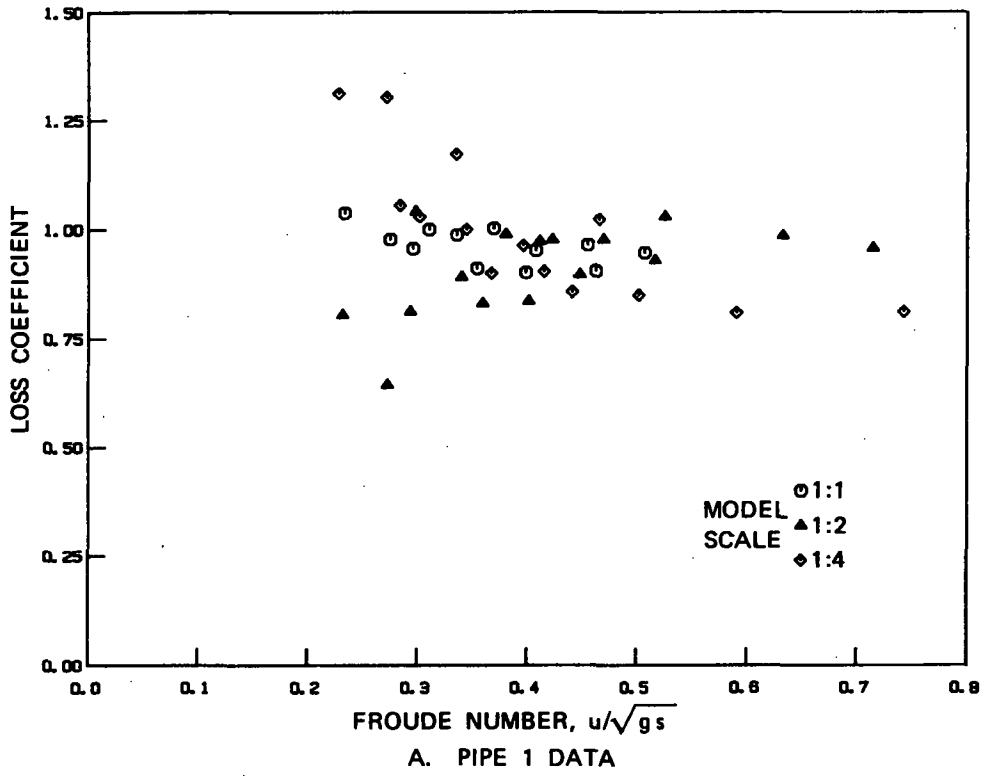


FIGURE 21 INLET LOSS COEFFICIENT VERSUS FROUDE NUMBER; UNIFORM APPROACH FLOW; BOTH PIPES OPERATING

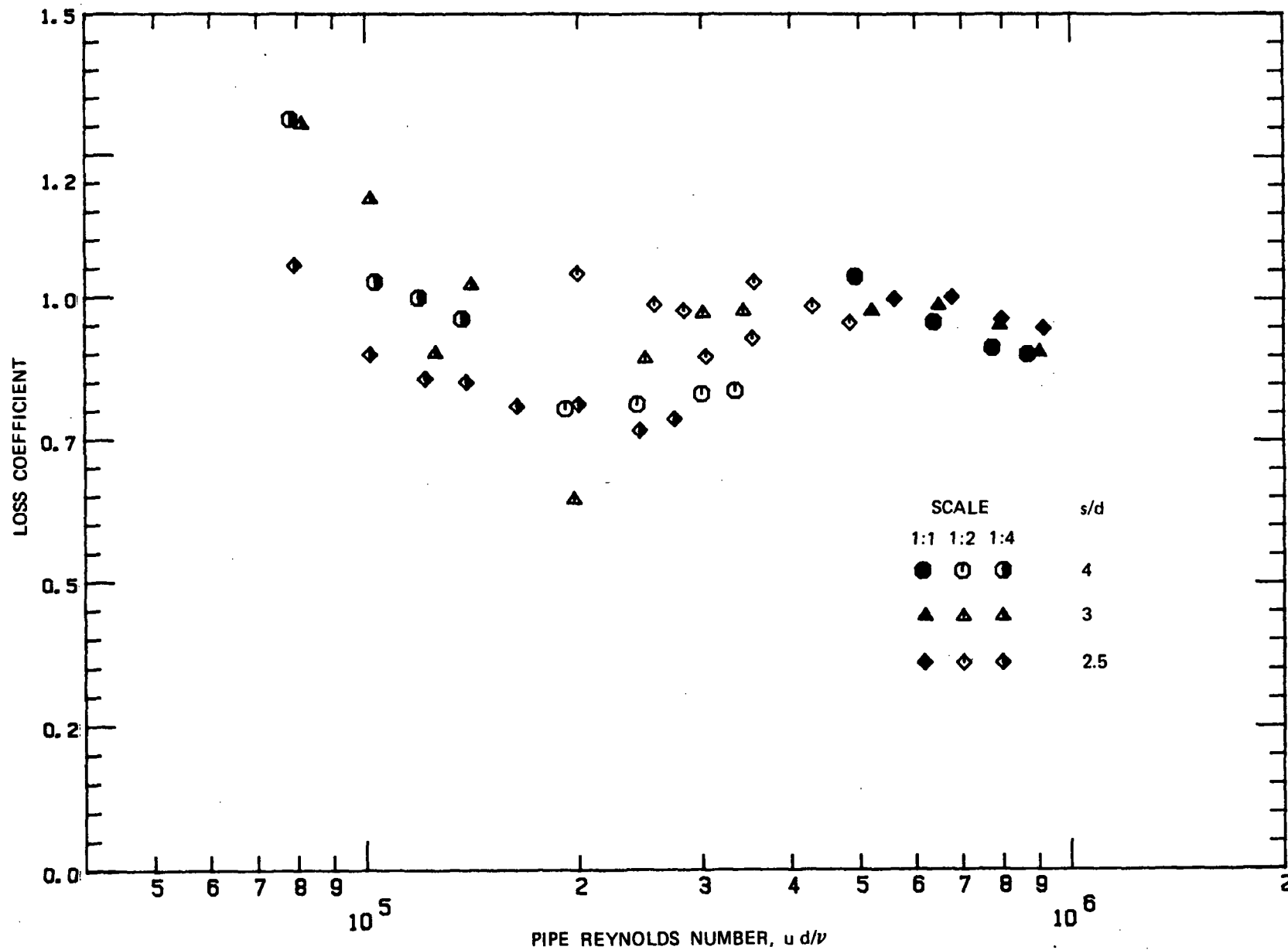


FIGURE 22 INLET LOSS COEFFICIENT VARIATION WITH PIPE REYNOLDS NUMBER;
 ... UNIFORM APPROACH FLOW; PIPE 1 DATA

increased somewhat when the pipe Reynolds number was below 10^5 . As shown in Figure 23, such a trend was also observed for screen blockage scheme 2. However, for one pipe operation case, no Reynolds number influence was observed, as illustrated in Figure 24. The reason for this is not clear, except that the flow patterns at the vicinity of the pipe entrance could be different in this case compared to both pipes operating.

In general, maintaining the pipe Reynolds numbers higher than 10^5 in a reduced scale model would allow more accurate evaluation of the loss coefficient. This finding is supportive of some investigations (19) involving closed conduit flows which indicate that if the requirement of Euler scaling criterion is to be satisfied in a model (which is a requirement for identical pressure loss coefficients in the model), the duct Reynolds numbers should be kept above 10^5 . For the present case, this Re requirement is not very important since the loss coefficient is conservatively predicted at lower Reynolds numbers.

4.5 Blockage Tests With No Screens and Gratings in the Unblocked Screen Area

The results of blockage tests using scheme 2, but with no screens and gratings in the open area, are indicated in Figure 25. Since these results support the findings reported in earlier sections, no apparent influence of modeling the screen and grating on the outcome of the study is indicated. However, it should be pointed out that without the screens and gratings, the approach flow into the sump produced surface waves and surface eddies (both in the full scale and model sumps) which contributed towards more unsteady vortices compared to the case with screens and gratings. Hence, if the full scale sump has screens and gratings, a proper simulation of vortexing in a reduced scale model requires properly simulated screens and gratings.

4.6 Envelope Curves

From the Phase I test data on several full scale sump configurations with 12 inch diameter horizontal outlets, certain envelope curves are derived and presented in (7). Specifically, these curves were considered useful in prescribing upper bounds of air-withdrawals due to vortices, average vortex types, pipe swirl, and inlet losses.

Model and full scale test data on average vortex types and void fractions from this study are compared to the envelope plots of Phase I (full scale; horizontal dual outlets), and the results are shown in Figures 26 and 27. Most of the average vortex type data and all of the void fraction data fall within the maximum envelopes developed in Phase I.

Regarding swirl angles, values up to 8.8 degrees (converted to a location at about 14.5 pipe diameters from the entrance) were observed in the model and full scale for the selected sump, while Phase I tests with 12

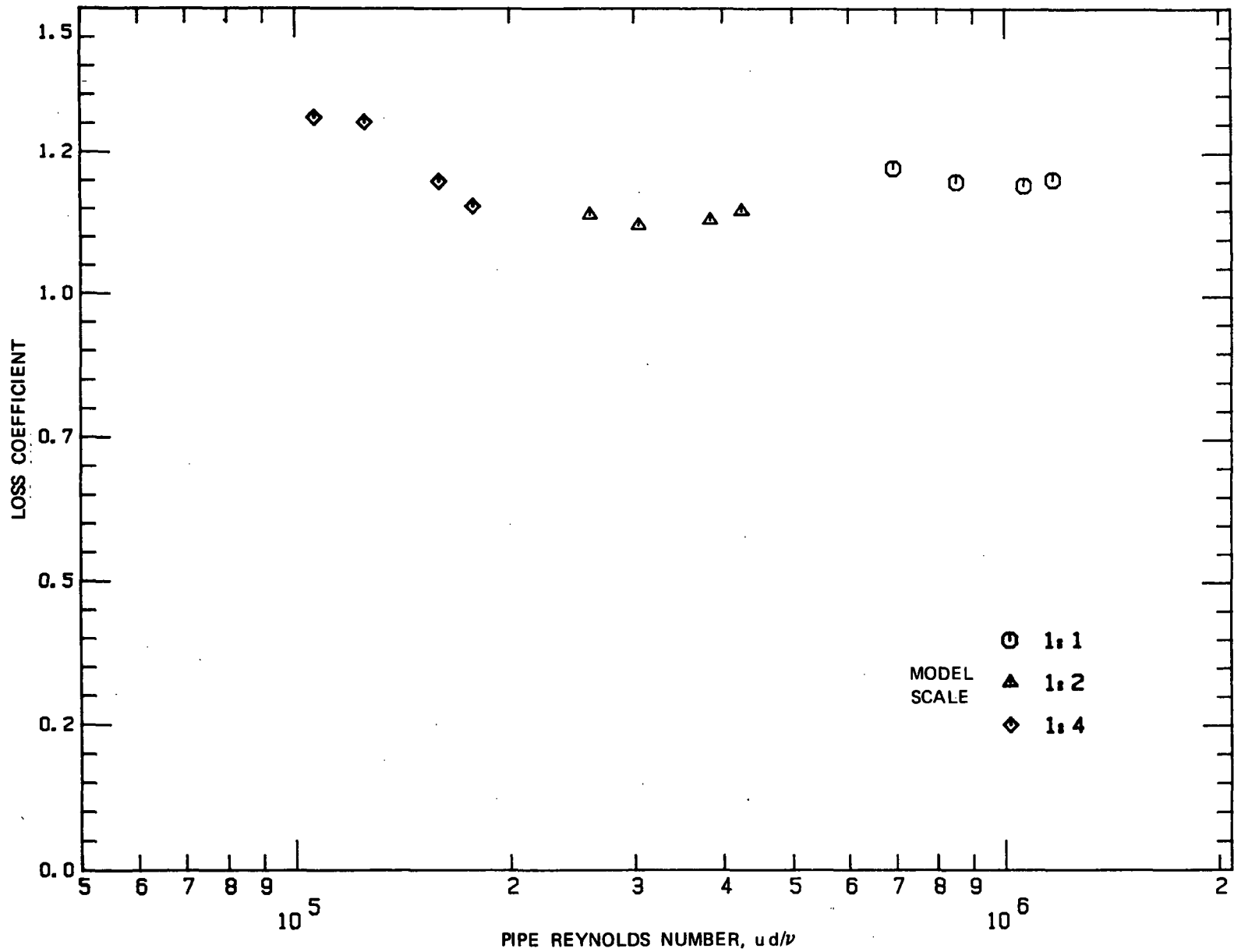
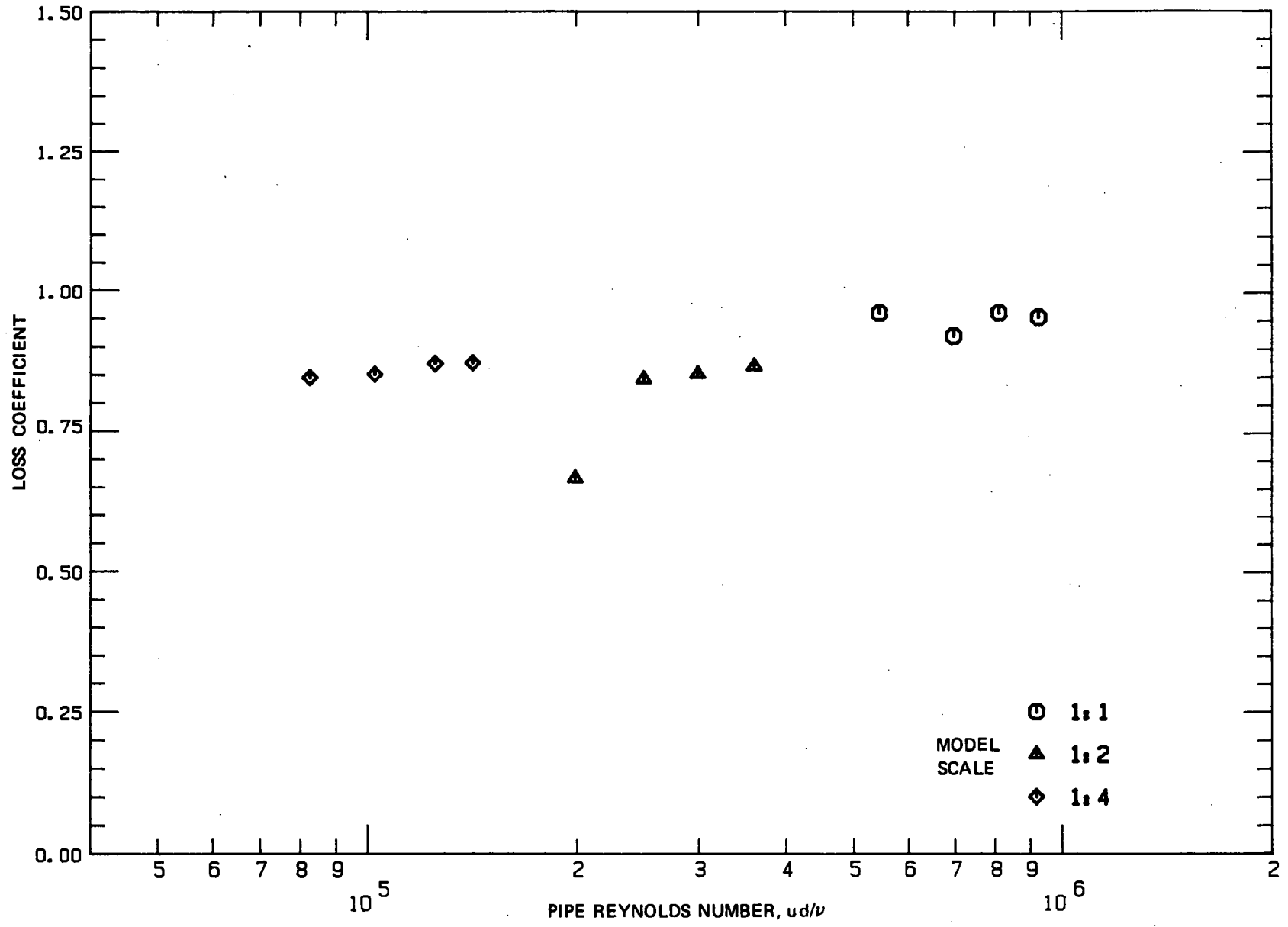
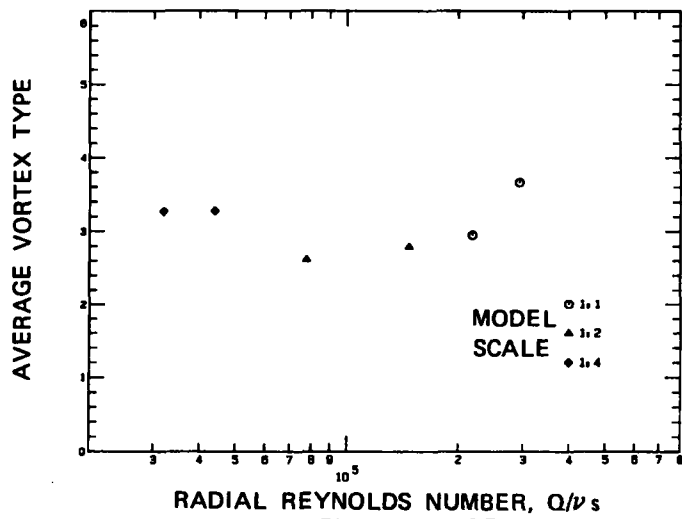


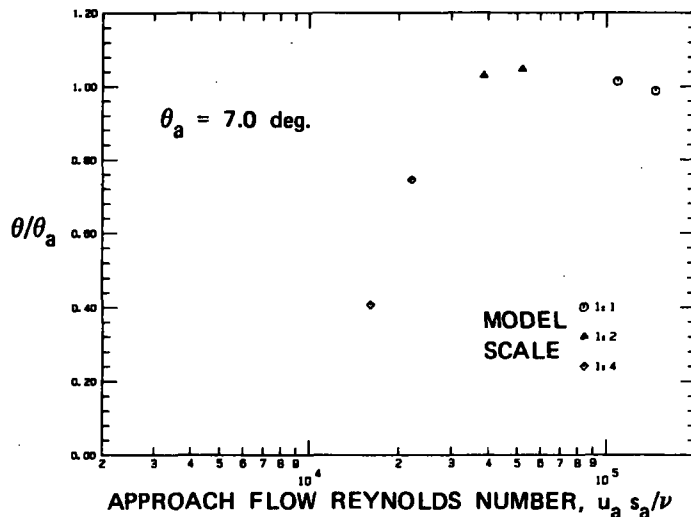
FIGURE 23 INLET LOSS COEFFICIENT VERSUS PIPE REYNOLDS NUMBER;
 SCREEN BLOCKAGE SCHEME 2; $s/d = 2.5$; PIPE 2



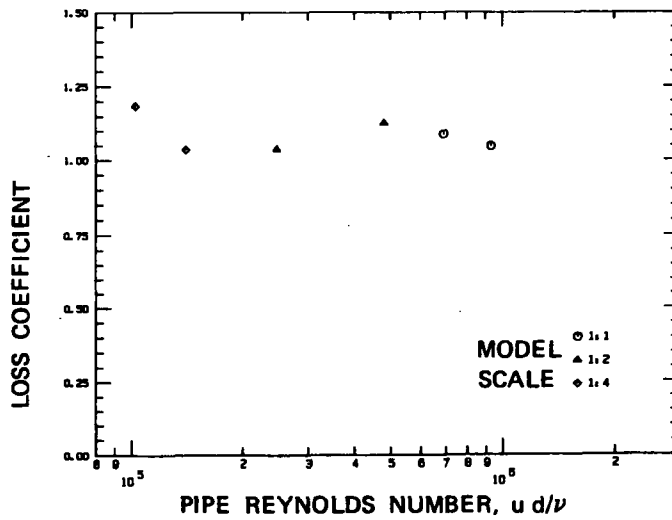
**FIGURE 24 INLET LOSS COEFFICIENT VARIATION WITH PIPE REYNOLDS NUMBER;
ONE PIPE OPERATING; $s/d = 2.5$**



A. VORTEX TYPE VARIATION WITH REYNOLDS NUMBER



B. SWIRL ANGLE VARIATION WITH REYNOLDS NUMBER



C. INLET LOSS COEFFICIENT VARIATION WITH REYNOLDS NUMBER

FIGURE 25 RESULTS OF TESTS WITH NO SCREENS AND GRATINGS IN OPEN PORTION OF SCHEME 2 BLOCKAGE

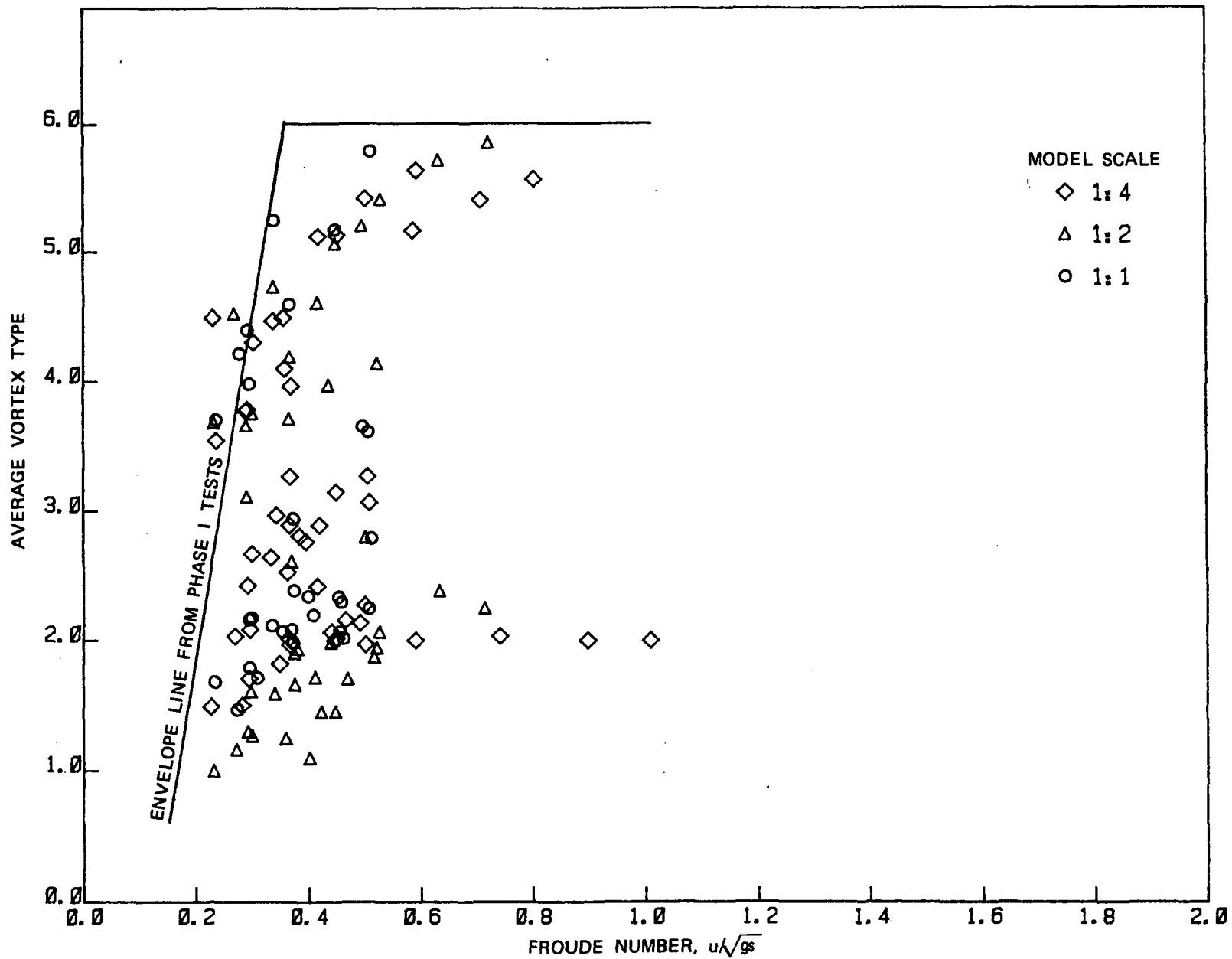


FIGURE 26 AVERAGE VORTEX TYPE DATA COMPARED WITH RESPECT TO ENVELOPE LINE FROM PHASE I, TESTS(7)

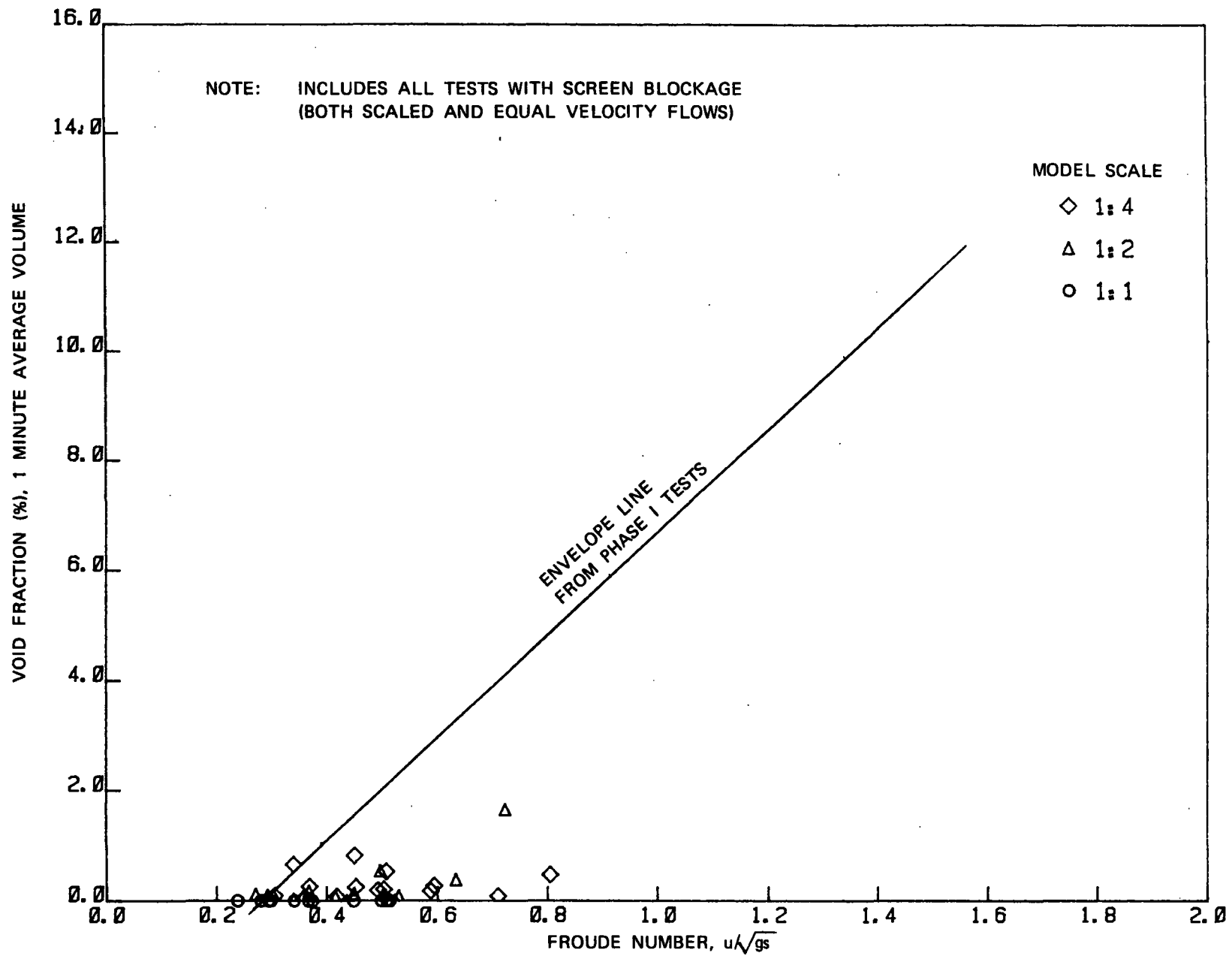


FIGURE 27 VOID FRACTION DATA COMPARED WITH RESPECT TO ENVELOPE LINE FROM PHASE I, TESTS (7)

inch pipe showed values to about 5 degrees for the same Froude number range. Additional tests of other sump configurations with 24 inch outlet also showed higher swirl levels than the Phase 1 tests with 12 inch outlets (22). The loss coefficients in general were within the ranges found in Phase I; namely, 0.8 ± 0.2 .

4.7 General

Large geometric scale models (1:4 scale or larger) of sumps operated based on Froude similitude criteria are demonstrated by this study to provide a reliable means of predicting the hydraulic performance of containment recirculation sumps if the models are designed such that the model operating ranges fall above certain limiting values of appropriate non-dimensional numbers, such as Reynolds and Weber numbers. The limiting values derived from this study, together with the use of available literature on free-surface vortexing (10, 11, 12, 20), may be used to assure the reliability of results obtained from reduced scale model studies conducted in the past. In general, the findings of this study support the use of reduced scale hydraulic models of scales 1:4 and larger in verifying sump performance by both utilities responsible for the power stations and the regulatory authorities responsible for licensing.

REFERENCES

1. Murakami, M., et al, "Flow of Entrained Air in Centrifugal Pumps," 13th Congress, IAHR, Japan, August 31-September 5, 1969.
2. Patel, B.R., and Runstadler, Jr., P.W., "Investigations into the Two-Phase Flow Behavior of Centrifugal Pumps", Polyphase Flow in Turbo Machinery, ASME Winter Annual Meeting, San Francisco, California, December 1978.
3. Florajancic, D., "Influence of Gas and Air Admission on the Behavior of Single and Multi-Stage Pumps", Sulzer Research Number, 1970.
4. Nystrom, J.B., Padmanabhan, M., and Hecker, G.E., "Flow Characteristics of Reactor Residual Heat Removal Sumps", Joint Power Generation Conference, ASME/IEEE/ASCE, St. Louis, Missouri, October 1981.
5. Padmanabhan, M., "Assessment of Flow Characteristics Within a Reactor Containment Recirculation Sump Using a Scale Model", McGuire Nuclear Power Station, ARL Report No. 29-78, May 1978.
6. Padmanabhan, M., "Containment Sump Reliability Studies (Generic Task A-43) - Interim Report on Test Results", ARL Report No. 59-81, June 1981.
7. "A Parametric Study of Containment Emergency Sump Performance", Joint ARL/Sandia Report, ARL/46-82, SAND/82-0624, NUREG/CR2758, 1982.
8. "Results of Vertical Outlet Sump Tests", Joint ARL/Sandia Report, ARL/47-82, SAND/82-1286, NUREG/CR-2759, 1982. (to be published)
9. Rouse, H., Handbook of Hydraulics, John Wiley & Sons, 1950.
10. Daggett, L.L., and Keulegan, G.H., "Similitude Conditions in Free Surface Vortex Formations", Journal of Hydraulics Division, ASCE, Vol. 100, pp. 1565-1581, November 1974.
11. Anwar, H.O., Weller, J.A., and Amphlett, M.B., "Similitude of Free Vortex at Horizontal Intake," Journal of Hydraulic Research, IAHR 16, No. 2, 1978.
12. Jain, A.K., et al., "Vortex Formation at Vertical Pipe Intakes," Journal of Hydraulic Division, ASCE, August 1978.
13. Zielinski, P.B., and Villemonte, J.R., "Effect of Viscosity on Vortex-Orifice Flow," Journal of Hydraulics Division, ASCE, May 1968.

14. Baines, W.D., and Peterson, E.G., "An Investigation of Flow Through Screens," Trans. ASME, pp. 467-477, July 1951.
15. Padmanabhan, M., and Vigander, S., "Pressure Drop Due to Flow Through Fine Mesh Screens," Journal of Hydraulics Division, ASCE, August 1978.
16. Padmanabhan, M., and Janik, C.R., "Swirling Flow and its Effect on Wall Pressure Drop Within Pipes," Symposium on Vortex Flows, The Winter Annual Meeting of ASME, Chicago, Illinois, November 1980.
17. Wolf, L., Lavan, Z., and Fejer, A.A., "Measurement of the Decay of Swirl in Turbulent Flow," AIAA Journal, Vol 7, May 1969.
18. Reddy, Y.R., and Pickford, J.A., "Swirl Angle Distribution in Pump Inlets in a Circular Sump," Pumps 1979, 6th Technical Conference of British Pump Manufacturer's Association, Canterbury, England, March 28-30, 1979.
19. March, P.A., "Velocity Distributions and Turbulence Intensities at Tubesheets in a Two-Pass Condenser Model," Transactions of the ASME, Vol. 101, July 1979.
20. Hecker, G.E., "Model-Prototype Comparison of Free Surface Vortices," Journal of the Hydraulics Division, ASCE, Vol. 107, No. HY10, October 1981.
21. Durgin, W.W., Padmanabhan, M., and Janik, C.R., "The Experimental Facility for Containment Sump Reliability Studies," ARL Report No. 120-80, December 1980.
22. Padmanabhan, M., "Results of Vortex Suppressor Tests, Single Outlet Sump Tests, and Miscellaneous Sensitivity Tests", ARL Report No. 49-82/M398F Also, NUREG/CR-2761, 1982. (to be published)
23. "Containment Emergency Sump Performance", Resolution of Unresolved Safety Issue A-43, U.S. Nuclear Regulatory Commission, NUREG-0897, 1982.

APPENDIX A

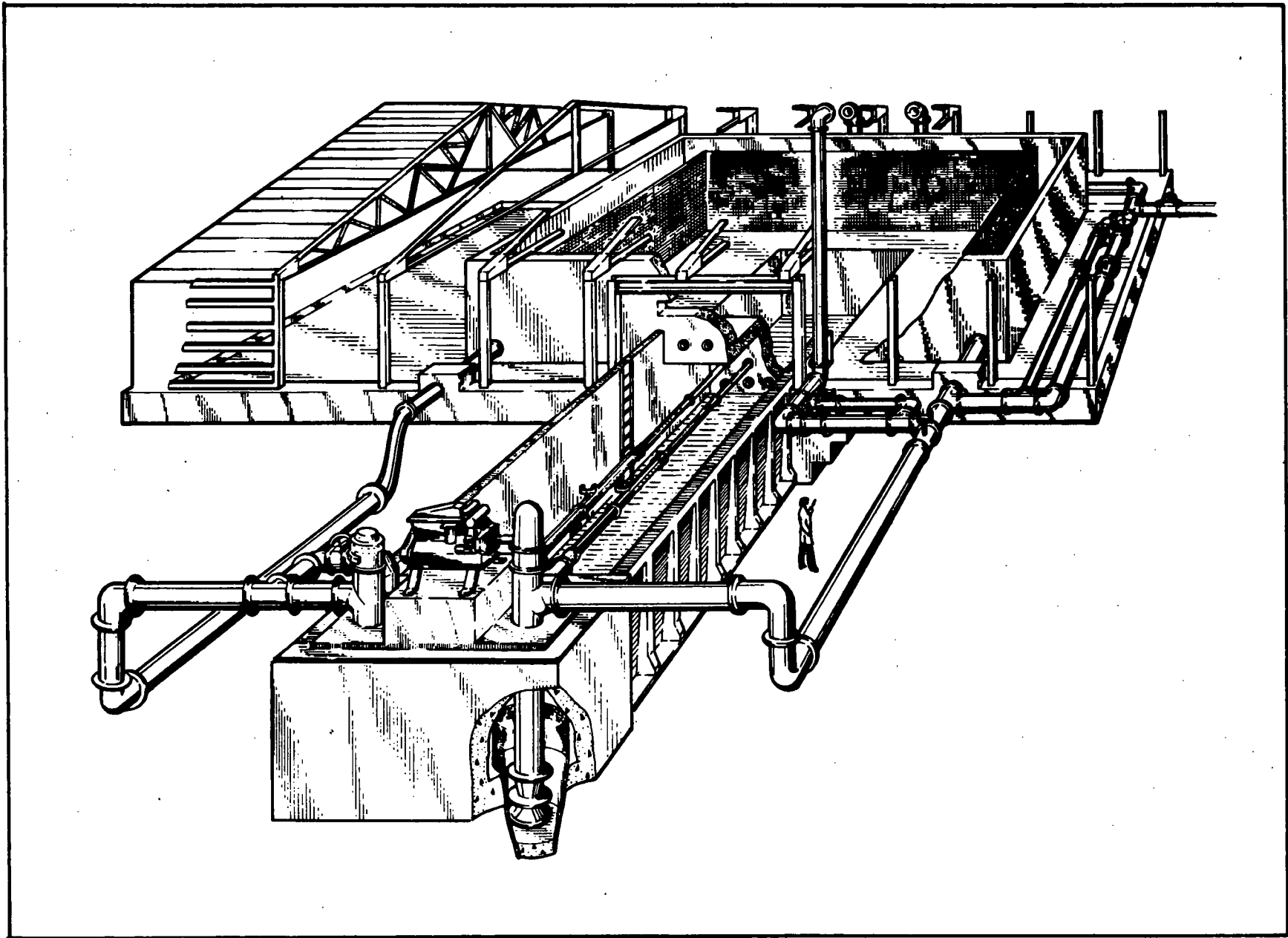
FACILITY, MEASUREMENTS TECHNIQUES, AND DATA ACQUISITION

Detailed descriptions of the facility, instrumentation, measurement techniques, and data acquisition are given in references (6, 7, 8). However, brief descriptions to explain the facility operation and the techniques and locations of the measurements of swirl, void fraction, and pressure gradient are included in here.

An isometric sketch, plan, and sections of the facility are shown in Figures A1 and A2. The test facility was designed so that any of the flow or geometric parameters of the sump could be varied over typical ranges with least time and effort by simple alterations of floors, walls, and pipe fittings. The facility consists of a concrete main tank, 70 ft by 35 ft by 12.5 ft, and a concrete sump tank, 20 ft by 15 ft by 10 ft, situated within the main tank. Inflow was distributed along three sides of the main tank, and provision was made to produce non-uniform approach flows using blockage. False walls and tank floors were provided such that sump geometrics could be varied. Four rows of outlet holes in the front wall were provided with each row having five holes of 24 inch diameter at 4 ft centers. Sets of two holes in a row were used to attach the suction pipes which could be of any diameter in the range of 6 inches to 24 inches.

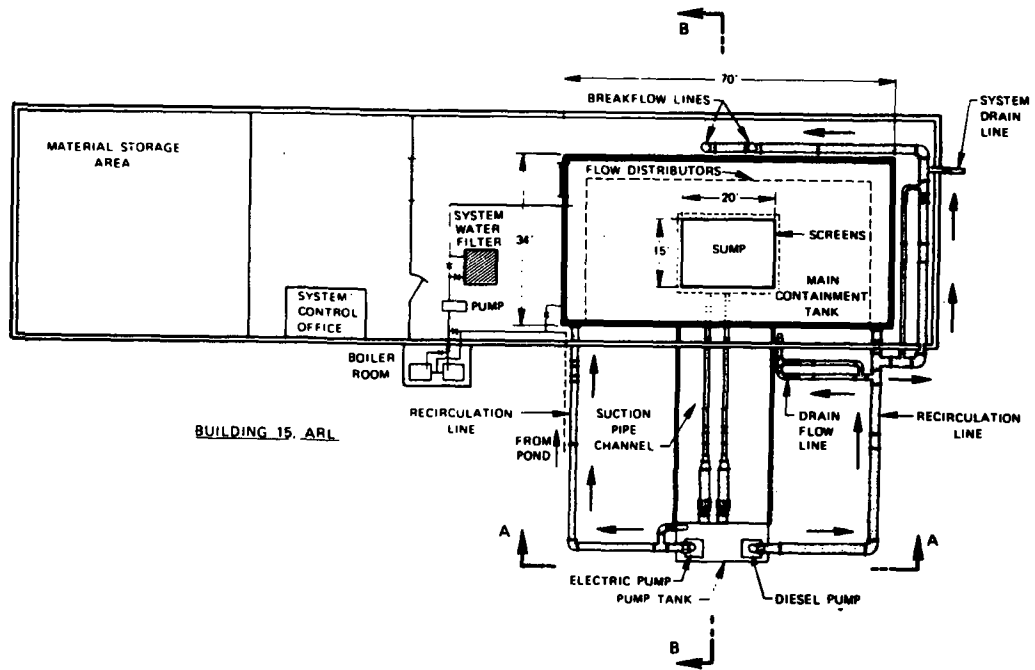
The suction pipes extend from the sump tank to a suction chamber 50 ft away and are long enough to facilitate swirl, pressure gradient, and discharge measurements. Each of the suction pipes accommodates a vortimeter for swirl measurement and ten pressure taps, one pipe diameter apart for pressure gradient measurements. Flow in the suction pipes can be remotely regulated and measured. The flow capacity was 20,000 gpm and up to 60% of the total flow could be delivered as breakflow and/or drain flow simulations.

A numerical scale is used to indicate the free-surface vortex types, with the graduations from "0" for no visible activity to "6" for a vortex with defined air core entering the inlet. Intermediate numerical values were assigned to discernible stages of development (see Figure A3). An observer entered the vortex type on a keypad at preselected intervals of 30 seconds. These data were then available for time series analysis in the acquisition system. Further documentation of the observations was achieved using photographs, movie, and video recordings. Pipeline swirl was indicated by crossed-vane swirl meters (Figure A4) commonly called vortimeters. These devices rotate about the pipe central axis and the vanes span about 75% of the cross-section. The inlet loss coefficients (includes screen and grating losses) were established by measuring the hydraulic gradeline at 1 minute intervals in the discharge lines and extrapolating the average hydraulic gradeline over a test back to the entrance. Ten piezometers were provided

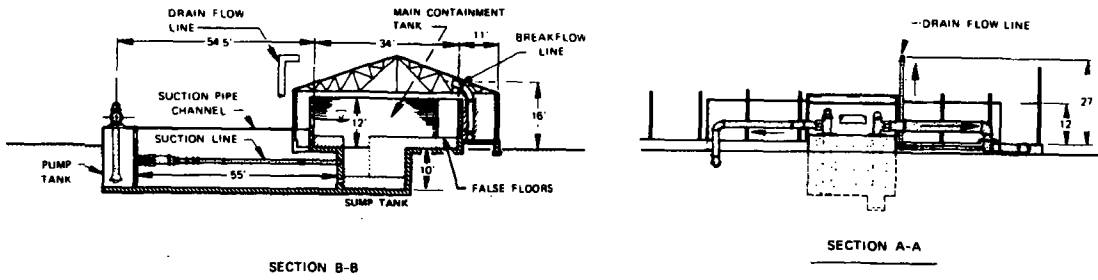


A2

FIGURE A1 PERSPECTIVE VIEW OF THE FACILITY



B PLAN OF FACILITY



D SECTIONAL VIEWS OF FACILITY

FIGURE A2 DETAILS OF THE FACILITY

**VORTEX
TYPE**

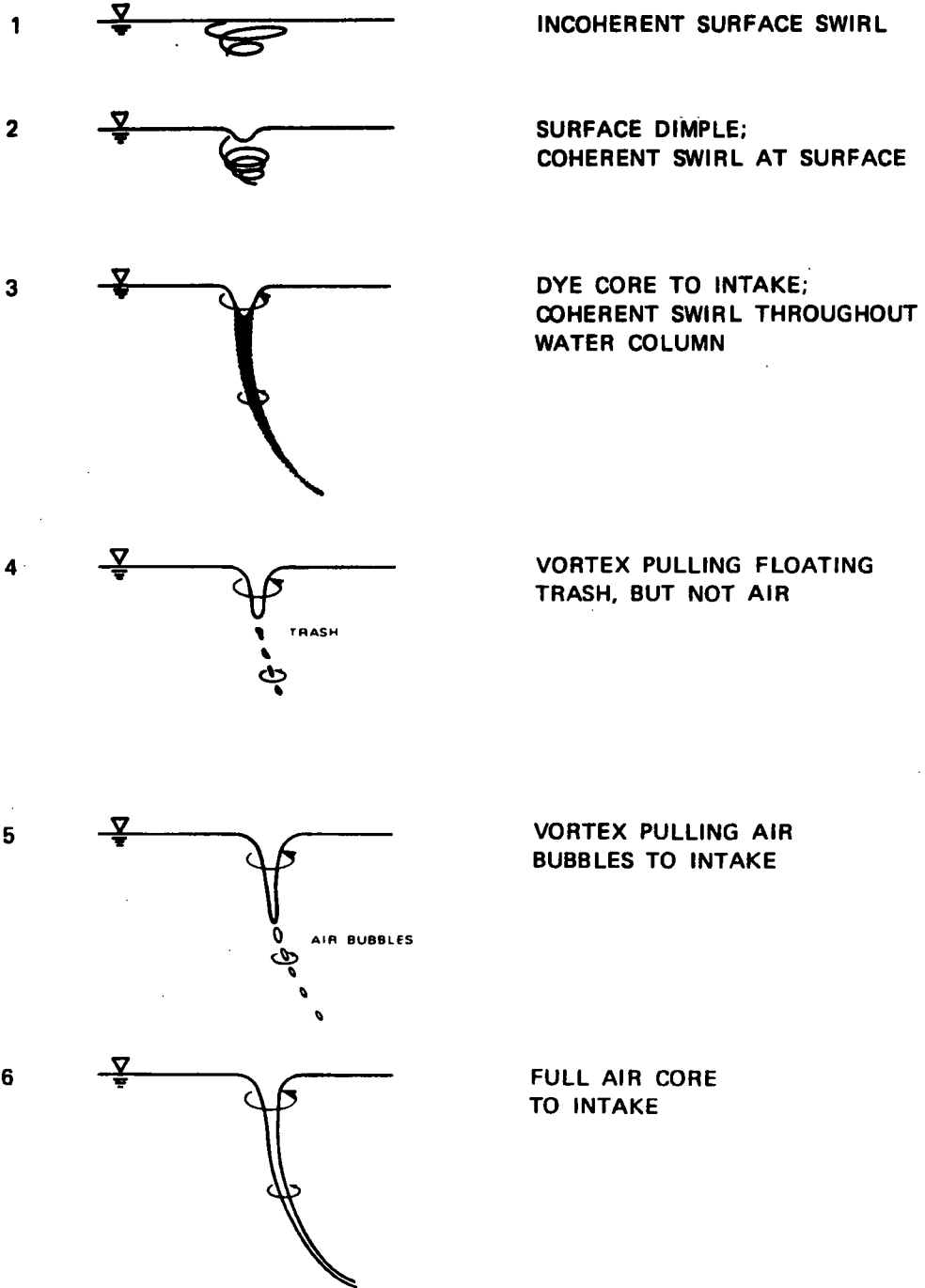


FIGURE A3 VORTEX TYPE CLASSIFICATION

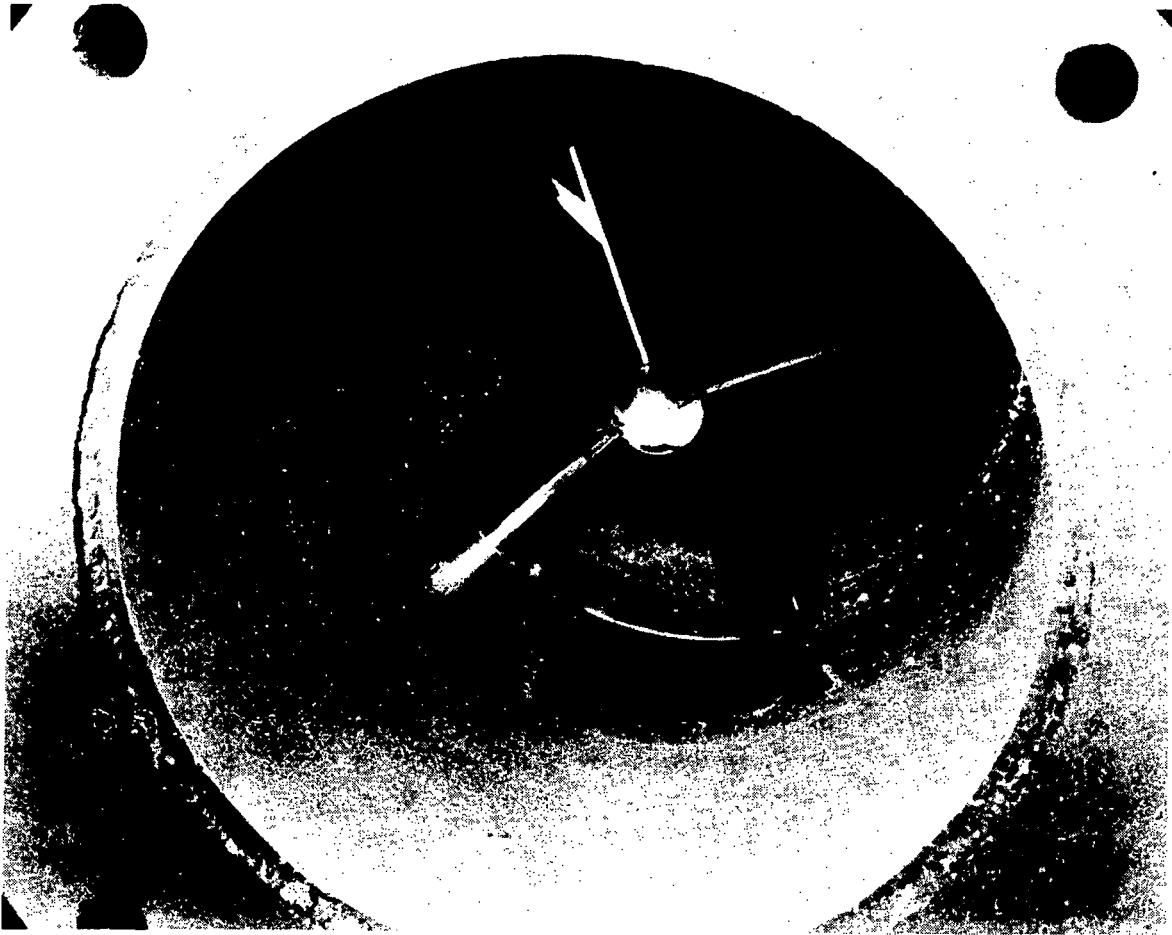


FIGURE A4 SWIRLMETER FOR 12" PIPE

in each line and individual locations were selected via a scanning valve control of the data acquisition system. The water depth outside the sump screens and grating was also measured with the scanning valve. Figure A5 explains the method of inlet loss coefficient determination. The void fraction due to air transported in each discharge line was determined using a conductivity meter of the rotating electric field type. The cross-sectional average conductivity was measured and was proportional to the volume of conductive component of the two-phase flow. The calibration data reported by the manufacturer for a range of void fractions of 0 to 20 percent indicated a standard deviation of about 1 percent void fraction.

A mini-computer based data acquisition system was used to record measurements and observations for each test, as shown in Figure A6. At intervals of 30 seconds, an observer entered the vortex type and location using a small terminal and for the same interval, the system counted the number and direction of vortimeter revolutions in each test line. The pressure taps for pressure gradients were monitored for five seconds each including some allowance for settling and averaging of the signal. With two auxiliary pressure measurements for each system, the gradeline for each pipe was established every 60 seconds. A similar pressure scanning system was used to monitor seven differential flow meters on a 30 second cycle. The analog output from the void fraction meters was sampled every 5 seconds and the water temperature sampled every 30 seconds. The data were displayed on a video terminal in suitable formats to aid the operators in setting up test runs. At the end of each test run, all data were transferred to disc files for storage and further processing and display.

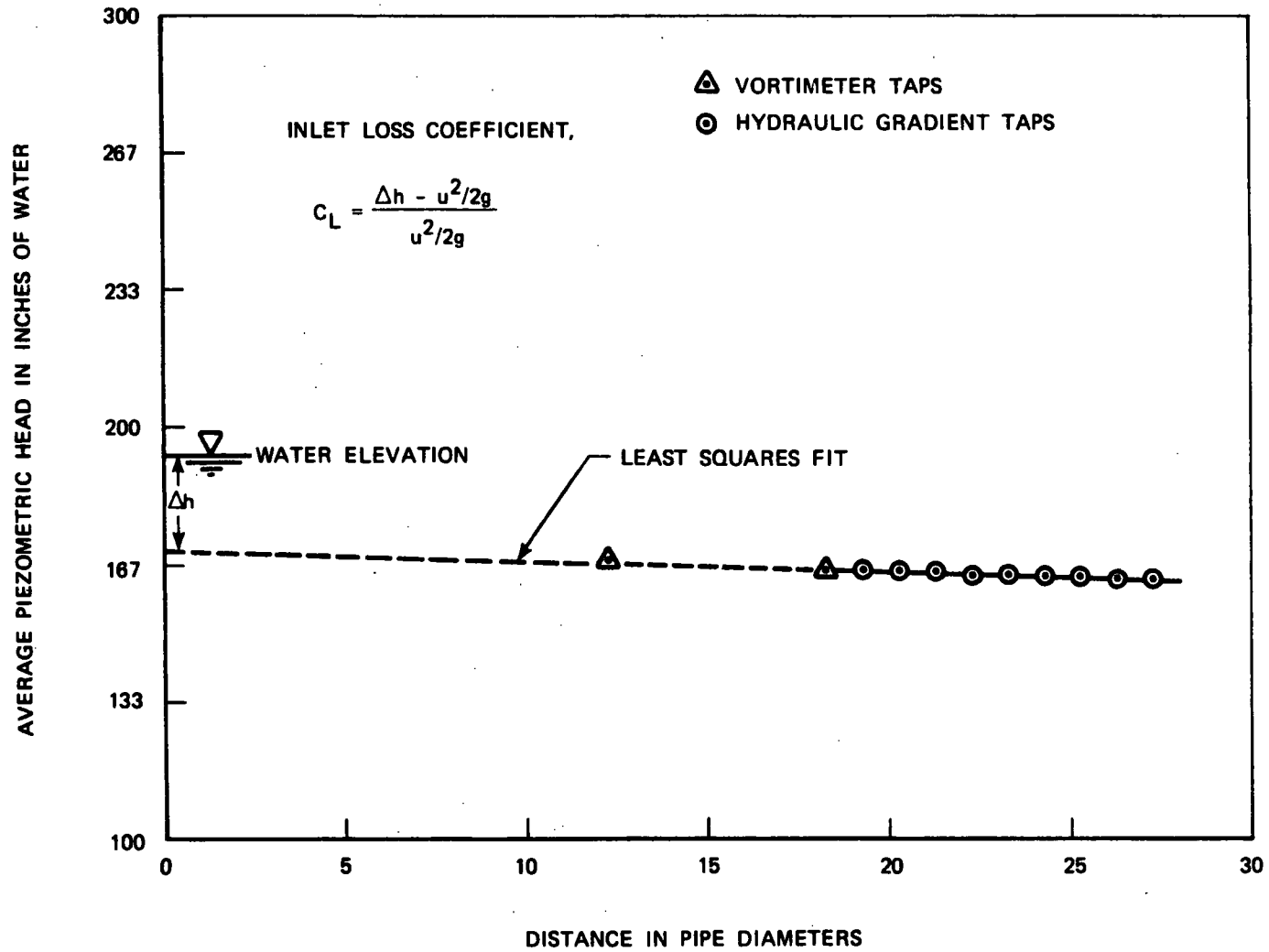


FIGURE A5 INLET LOSS COEFFICIENT DETERMINATION

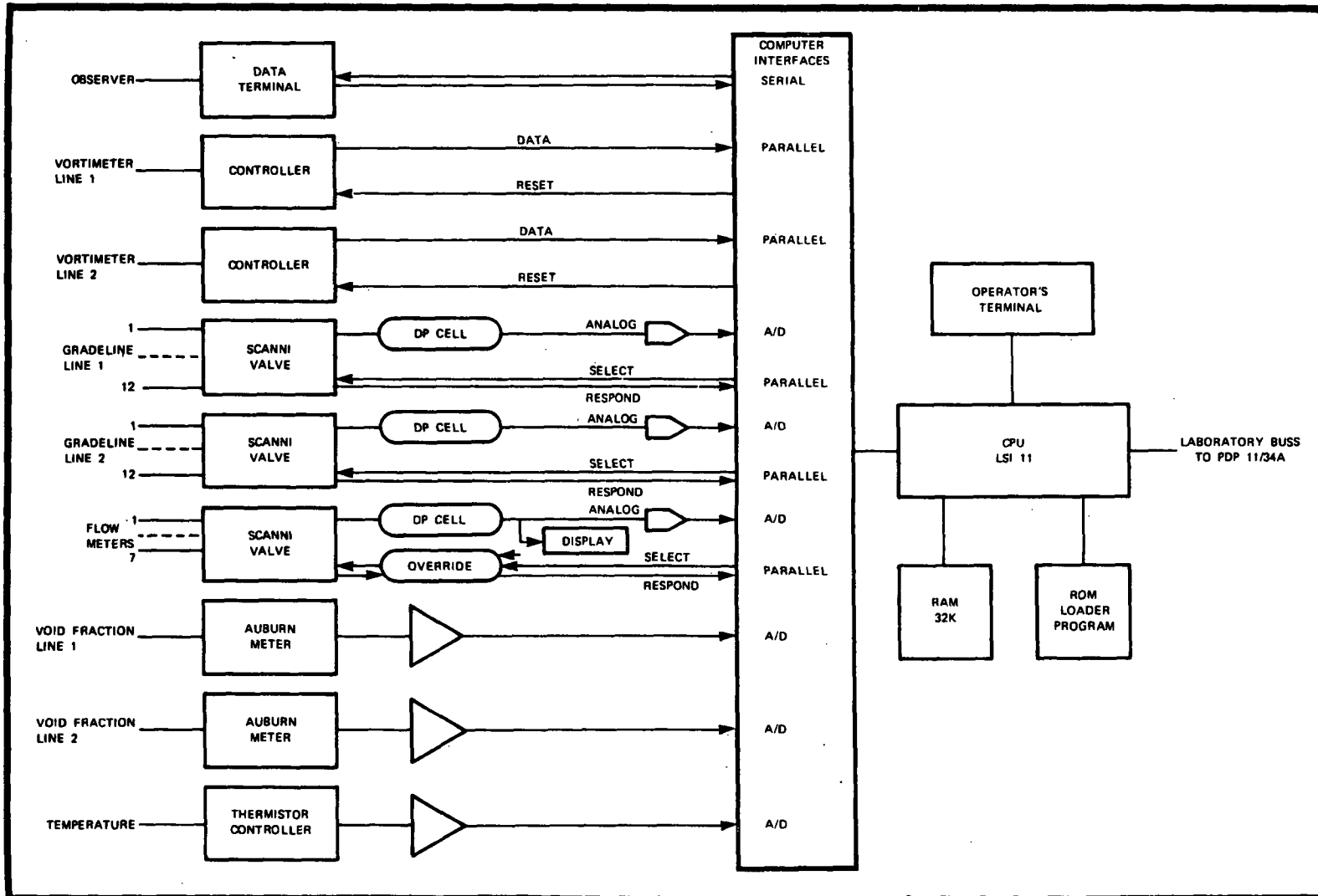


FIGURE A6 DATA ACQUISITION SCHEME

APPENDIX B

MODEL SIMILITUDE

The study of dynamically similar fluid motions forms the basis for the design of models and the interpretation of experimental data. The basic concept of dynamic similarity may be stated as the requirement that two systems with geometrically similar boundaries have geometrically similar flow patterns at corresponding instants of time (9). Thus, all individual forces acting on corresponding fluid elements of mass must have the same ratios in the two systems.

The condition required for complete similitude may be developed from Newton's second law of motion:

$$F_i = F_p + F_g + F_v + F_t \quad (1)$$

where

- F_i = inertia force, defined as mass, M , times the acceleration, a
- F_p = pressure force connected with or resulting from the motion
- F_g = gravitational force
- F_v = viscous force
- F_t = force due to surface tension

Additional forces may be relevant under special circumstances, such as fluid compression, magnetic or Coriolis forces, but these had no influence on this study and were, therefore, not considered in the following development.

Equation (1) can be made dimensionless by dividing all the terms by F_i . Two systems which are geometrically similar are dynamically similar if both satisfy the dimensionless form of the equation of motion, Equation (1). We may write each of the forces of Equation (1) as:

$$F_p = \text{net pressure} \times \text{area} = \alpha_1 \Delta p L^2$$

$$F_g = \text{specific weight} \times \text{volume} = \alpha_2 \gamma L^3$$

$$F_v = \text{shear stress} \times \text{area} = \alpha_3 \mu \Delta u / \Delta y \times \text{area} = \alpha_3 \mu u L$$

$$F_t = \text{surface tension} \times \text{length} = \alpha_4 \sigma L$$

$$F_i = \text{density} \times \text{volume} \times \text{acceleration} = \alpha_5 \rho L^3 u^2 / L = \alpha_5 \rho u^2 L^2$$

where

α_1, α_2 , etc. = proportionality factors
 L = representative linear dimension
 Δp = net pressure
 γ = specific weight
 μ = dynamic viscosity
 σ = surface tension
 ρ = density
 u = representative velocity

Substituting the above terms in Equation (1) and making it dimensionless by dividing by the inertial force, we obtain

$$\frac{\alpha_1}{\alpha_5} E^{-2} + \frac{\alpha_2}{\alpha_5} F^{-2} + \frac{\alpha_3}{\alpha_5} R^{-1} + \frac{\alpha_4}{\alpha_5} W^{-2} = 1 \quad (2)$$

where

$$E = \frac{u}{\sqrt{\Delta p/\rho}} = \text{Froude number} \propto \frac{\text{Inertia Force}}{\text{Pressure Force}}$$

$$F = \frac{u}{\sqrt{gL}} = \text{Froude number} \propto \frac{\text{Inertia Force}}{\text{Gravity Force}}$$

$$R = \frac{uL}{\mu/\rho} = \text{Reynolds number} \propto \frac{\text{Inertia Force}}{\text{Viscous Force}}$$

$$W = \frac{u}{\sqrt{\sigma/\rho L}} = \text{Weber number} \propto \frac{\text{Inertia Force}}{\text{Surface Tension Force}}$$

Since the proportionality factors, α_i , are the same in model and prototype, complete dynamic similarity is achieved if all the dimensionless groups, E , F , R , and W , have the same values in model and prototype. In practice, this is difficult to achieve. For example, to have the values of F and R the same requires either a 1:1 "model" or a fluid of very low kinematic viscosity in the reduced scale model. Hence, the accepted approach is to select the predominant force and design the model according to the appropriate dimensionless group. The influence of the other forces would be secondary and are called scale effects (9).

B.1 Froude Scaling

Models involving a free surface are constructed and operated using Froude similarity since the flow process is controlled by gravity and inertia forces. The Froude number, representing the ratio of inertia to gravitational force,

$$F = u/\sqrt{gs} \quad (3)$$

where

u = average velocity in the pipe
 g = gravitational acceleration
 s = submergence

is, therefore, made equal in model and prototype.

$$F_r = F_m / F_p = 1 \quad (4)$$

where m, p, and r denote model, prototype, and ratio between model and prototype, respectively.

From Equations (3) and (4), using $s_r = L_r$, the velocity, discharge, and time scales are:

$$u_r = L_r^{0.5} \quad (5)$$

$$Q_r = L_r^2 u_r = L_r^{2.5} \quad (6)$$

$$t_r = L_r^{0.5} \quad (7)$$

B.2 Similarity of Vortex Motion

The fluid motions involving vortex formation in the sumps of low head pump intakes have been studied by several investigators (10, 11, 12, 13). Anwar et al (11) have shown by principles of dimensional analysis that the dynamic similarity of fluid motion in an intake is governed by the dimensionless parameters given by

$$\frac{u}{\sqrt{2gs}}, \frac{Q}{v s}, \frac{\rho u^2 s}{\sigma}, \frac{s}{d}, \text{ and } \frac{c}{d}$$

where

Q = discharge through the outlet
 u = average velocity in the outlet pipe
 s = submergence
 d = diameter of the outlet pipe
 c = distance of pipe from floor
 v = kinematic viscosity of fluid

The influence of viscous effects was defined by the parameter $Q/(v s)$, known as a radial Reynolds number, R_r , and that of surface tension effects by the parameter, $\rho u^2 s / \sigma$, known as Weber number, W_s .

B.3 Scale Effects on Vortices

Viscous and surface tension forces could influence the formation and strength of vortices (10,11,12,13). The relative magnitude of these forces on the fluid inertia force is reflected in the Reynolds and Weber numbers, respectively.

For similarity between the dimensions of a vortex of types up to and including the narrow air-core type, it was shown that the viscous effects become negligible if $Q/(V s)$ was greater than 3×10^4 and the surface tension effects become negligible for W_s greater than 10^4 (11). As strong vortices are considered undesirable, the main concern for interpretation of prototype performance based on the model performance would be on the similarity of vortices. If viscous and surface tension forces have only a negligible role in a model, dynamic similarity is obtained by equalizing the parameters $u/\sqrt{2gs}$, s/d , and c/d in model and prototype. A Froude model would satisfy this condition, provided the approach flow pattern in the vicinity of the sump is properly simulated, which usually requires a large size model.

Referring to Daggett and Keulegan (10), the viscous effects on vortexing would be negligible if the pipe Reynolds number, $Re = ud/\nu$, is greater than 3×10^4 in the model. Using liquids of the same viscosity but different surface tension coefficients ($\sigma = 4.9 \times 10^3$ lb/ft to 1.15×10^3 lb/ft), it was shown that no surface tension effects were observed on vortexing (10). Jain et al (12) defined a Weber number (W_d) as $\rho u^2 d / \sigma$ and showed that above a Weber number of 120, surface tension effects are negligible. They showed that for a Froude number of about 1, the effects to the viscous forces on vortexing would be negligible for pipe Reynolds numbers of about 5×10^4 or higher. Zielinski and Villemonte (13) found from their experiments that viscous effects are negligible when pipe Reynolds number is greater than 10^4 .

B.4 Similarity of Flow Through Gratings

Gratings would have a guiding effect on the approach flow, especially if the grating bars are deep and are placed vertically oriented. Geometric scaling of depths and spacings of the grating bars would be sufficient to model any such flow guiding effect and to simulate the approach flow into the sump. The thickness of grating bars are scaled, if practical; otherwise made as close as possible.

B.5 Similarity of Flow Through Screens

In addition to providing protection from debris, screens tend to suppress non-uniformities of the approach flow. The aspects of flow through screens of concern in a model study are: (1) energy loss of the fluid passing through the screen, (2) modification of velocity profile and the deflection of streamlines at the screen, and (3) production of turbulence. As all these factors could affect vortex formation in a sump with approach flow directed through screens, a proper modeling of screen parameters is important.

The loss of energy across the screen occurs at a rate proportional to the drop in pressure, and this loss dictates the effectiveness of the screen in altering velocity profiles. The pressure drop across the screen is analogous

to the drag induced by a row of cylinders in a flow field and could be expressed in terms of a pressure-drop coefficient K (or alternately a drag coefficient), defined as (14,15),

$$K = \frac{\Delta p}{1/2 \rho u_a'^2} = \frac{\Delta H}{u_a'^2/2g} \quad (8)$$

where

Δp = drop in pressure across the screen
 u_a' = mean velocity of approach flow upstream of screens
 ρ = density of the fluid
 ΔH = head loss across the screen
 g = acceleration due to gravity

From the available literature on the topic (14,15), it may be seen that

$$K = f(R_s, S', \text{Pattern}) \quad (9)$$

where

R_s = screen Reynolds number, $u_a' d_w / \nu$, d_w being the wire diameter of the screen
 S' = solidity ratio, equal to the ratio of closed area to total area of screen

If the solidity ratio and the wire mesh pattern are the same in the model and prototype screens, the corresponding values of K would only be a function of the screen Reynolds number. This is analogous to the coefficient of drag in the case of the circular cylinder. It is known that K becomes practically independent of R_s at values of R_s greater than about 1000 (14). However, for models with low approach flow velocity and with fine wire screens, it is necessary to ascertain the influence of R_s on K for both the model and prototype screens before selecting screens for the model which are to scale changes in velocity distribution.

Velocity modification equations relating the upstream velocity profile and downstream velocity profile have been derived based on different theories (14). Most of these indicate a linear relationship between the upstream velocity profile and downstream velocity profile, shape and solidity ratio of screen, and value of K . If the wire shape and solidity ratio are the same in the model and prototype screens, it is possible to select a suitable wire diameter to keep the values of K approximately the same for the model and prototype screens at the corresponding Reynolds number ranges. Identical velocity modifications would be produced by the respective screens if the loss coefficients were identical.

NRC FORM 335 (7-77)		U.S. NUCLEAR REGULATORY COMMISSION BIBLIOGRAPHIC DATA SHEET		1. REPORT NUMBER (Assigned by DDC) NUREG/CR-2760 ARE-48-82 SAND82-7063	
4. TITLE AND SUBTITLE (Add Volume No., if appropriate) Assessment of Scale Effects on Vortexing, Swirl, and Inlet Losses in Large Scale Sump Models				2. (Leave blank)	
7. AUTHOR(S) M. Padmanabhan and G. E. Hecker				3. RECIPIENT'S ACCESSION NO.	
9. PERFORMING ORGANIZATION NAME AND MAILING ADDRESS (Include Zip Code) Alden Research Laboratory Worcester Polytechnic Institute Holden, Massachusetts 01520				5. DATE REPORT COMPLETED MONTH May YEAR 1982	
Under subcontract to Sandia National Laboratories Albuquerque, NM 87185				6. DATE REPORT ISSUED MONTH June YEAR 1982	
12. SPONSORING ORGANIZATION NAME AND MAILING ADDRESS (Include Zip Code) Division of Safety Technology Office of Nuclear Reactor Regulation U.S. Nuclear Regulatory Commission Washington, DC 20555				6. (Leave blank)	
13. TYPE OF REPORT Formal Technical Report				7. (Leave blank)	
15. SUPPLEMENTARY NOTES				10. PROJECT/TASK/WORK UNIT NO.	
16. ABSTRACT (200 words or less) To verify the use of reduced scale hydraulic models of large scale ratios to demonstrate the performance of containment emergency sumps, a test program involving two geometric scale models (1:2 and 1:4) of a full size sump (1:1) was undertaken as a part of the total test program towards the resolution of Unresolved Safety Issue A-43, "Containment Emergency Sump Performance". The test results substantiated that hydraulic models of large scale such as 1:2 to 1:4 reliably predicted the sump hydraulic performance. No scale effects on vortexing or air-withdrawals were apparent within the tested prediction range for both models. However, a good prediction of pipe flow swirl and inlet loss coefficient was found to require that the approach flow Reynolds number and pipe Reynolds number be above certain limits. Based on the results of these tests, it is concluded that properly designed and operated, reduced scale hydraulic models of geometric scales 1:4 or larger can be used both by utilities and by regulatory agencies to prove the satisfactory hydraulic performance of sump designs.				11. CONTRACT NO. FIN A1296	
17. KEY WORDS AND DOCUMENT ANALYSIS				14. (Leave blank)	
17a. IDENTIFIERS/OPEN-ENDED TERMS				17a. DESCRIPTORS	
18. AVAILABILITY STATEMENT Unlimited				19. SECURITY CLASS (This report) unclassified	
20. SECURITY CLASS (This page) unclassified				21. NO. OF PAGES	
22. PRICE \$				22. PRICE \$	

**UNITED STATES
NUCLEAR REGULATORY COMMISSION
WASHINGTON, D.C. 20555**

**OFFICIAL BUSINESS
PENALTY FOR PRIVATE USE, \$300**

**FOURTH-CLASS MAIL
POSTAGE & FEES PAID
USNRC
WASH. D. C.
PERMIT No. G-62**